NMR IN BIOMEDICINE
NMR Biomed. 2006;**19**:142–164
Published online in Wiley InterScience (www.interscience.wiley.com). DOI:10.1002/nbm.1011

Review Article

Lipid-based nanoparticles for contrast-enhanced MRI and molecular imaging

Willem J. M. Mulder,[1]* Gustav J. Strijkers,[1] Geralda A. F. van Tilborg,[1] Arjan W. Griffioen[2] and Klaas Nicolay[1]

[1]Biomedical NMR, Department of Biomedical Engineering, Eindhoven University of Technology, P.O. Box 513, 5600 MB Eindhoven, The Netherlands
[2]Angiogenesis Laboratory, Research Institute for Growth and Development, Department of Pathology, Maastricht University and University Hospital, P.O. Box 5800, 6202 AZ Maastricht, The Netherlands

Received 18 July 2005; Revised 13 October 2005; Accepted 28 October 2005

ABSTRACT: In the field of MR imaging and especially in the emerging field of cellular and molecular MR imaging, flexible strategies to synthesize contrast agents that can be manipulated in terms of size and composition and that can be easily conjugated with targeting ligands are required. Furthermore, the relaxivity of the contrast agents, especially for molecular imaging applications, should be very high to deal with the low sensitivity of MRI. Lipid-based nanoparticles, such as liposomes or micelles, have been used extensively in recent decades as drug carrier vehicles. A relatively new and promising application of lipidic nanoparticles is their use as multimodal MR contrast agents. Lipids are amphiphilic molecules with both a hydrophobic and a hydrophilic part, which spontaneously assemble into aggregates in an aqueous environment. In these aggregates, the amphiphiles are arranged such that the hydrophobic parts cluster together and the hydrophilic parts face the water. In the low concentration regime, a wide variety of structures can be formed, ranging from spherical micelles to disks or liposomes. Furthermore, a monolayer of lipids can serve as a shell to enclose a hydrophobic core. Hydrophobic iron oxide particles, quantum dots or perfluorocarbon emulsions can be solubilized using this approach. MR-detectable and fluorescent amphiphilic molecules can easily be incorporated in lipidic nanoparticles. Furthermore, targeting ligands can be conjugated to lipidic particles by incorporating lipids with a functional moiety to allow a specific interaction with molecular markers and to achieve accumulation of the particles at disease sites. In this review, an overview of different lipidic nanoparticles for use in MRI is given, with the main emphasis on Gd–based contrast agents. The mechanisms of particle formation, conjugation strategies and applications in the field of contrast-enhanced, cellular and molecular MRI are discussed. Copyright © 2006 John Wiley & Sons, Ltd.

KEYWORDS: Lipid-based nanoparticles; contrast-enhanced magnetic resonance imaging; molecular imaging; micelles; liposomes; microemulsions

INTRODUCTION

Magnetic resonance imaging (MRI) is the most versatile imaging method available in both clinical and research settings. The signal of MRI is dependent on the longitudinal (T_1) and transverse (T_2) proton relaxation times of mainly water and therefore differences in proton relaxation times result in differences in contrast in MR images (1). The intrinsic relaxation times of tissue water are dependent on the physiological environment and may be altered in pathological tissue. This change may show little specificity and occur at a late stage of the disease. Therefore, a more specific and earlier detection of pathology with MRI is highly desirable. The relaxation times of tissue can be altered with contrast agents that decrease the longitudinal and transverse relaxation time. The ability of a contrast agent to shorten T_1 and T_2 is defined as the relaxivity (2), r_1 or r_2, and is expressed in $mM^{-1}\,s^{-1}$. In general, there are two classes of MR contrast agents. On the one hand, there are agents that have a low r_2/r_1 ratio and therefore generate positive contrast in T_1-weighted images. These positive contrast agents (3) usually are paramagnetic complexes of Gd^{3+} or Mn^{2+} ions. On the other hand, there are superparamagnetic contrast agents with a high r_2/r_1 ratio, which cause dark spots in T_2- and T_2*-weighted images and are therefore referred to as negative contrast agents (4). These contrast agents are usually based on iron oxide particles.

MRI applications are becoming more and more dependent on contrast agents. The combination of MRI and contrast agents greatly enhances the possibilities to depict the vascular system (5), inflamed tissue as in arthritis (6), tumor angiogenesis (7,8), atherosclerotic plaques (9,10) and the breakdown of the blood–brain barrier related to pathologies such as multiple sclerosis (11). Within the emerging field of cellular and molecular MRI, contrast agents have become an essential element of the technique.

**Correspondence to:* W. J. M. Mulder, Biomedical NMR, Department of Biomedical Engineering, Eindhoven University of Technology, P.O. Box 513, 5600 MB Eindhoven, The Netherlands.
E-mail: w.j.m.mulder@tue.nl

The aim of molecular and cellular MR imaging is to image non-invasively cellular and molecular events, usually related to pathology or transgene expression. Different imaging methods have already shown their capability to function as a molecular imaging modality (12). Nuclear methods such as PET and SPECT are especially interesting because of their high sensitivity. On the other hand, the spatial resolution of these modalities is low and the definition of anatomy is poor. MRI has good spatial resolution, but in order to become suitable as a molecular imaging modality the inherently low sensitivity has to be dealt with. This may be realized by using contrast agents with a very high relaxivity, e.g. by using nanoparticles containing a high payload of Gd complexes or using iron oxide particles with a high payload of iron.

Roughly, MR contrast agents can be divided into four groups or classes. The first group consists of *non-specific contrast agents* and includes both the low molecular weight contrast agents, e.g. Gd–DTPA, and the high molecular weight blood pool agents (13), such as high-generation dendrimers (14). These agents can be used for MR angiography and to measure the perfusion and permeability properties of tissue. The second class of molecules is *targeted contrast agents*, which are actively directed to a specific molecular target with an appropriate ligand. An early report of such a contrast agent by Sipkins *et al.* described the detection of tumor angiogenesis with an $\alpha v\beta 3$-specific antibody that was conjugated to polymerized paramagnetic liposomes (15). The third group consists of the so-called *smart contrast agents*, also referred to as activated or responsive agents. An example of such an agent is EgadMe, a complex which contains a sugar moiety that prevents water to coordinate with Gd^{3+}. Enzymatic cleavage of this sugar by β-galactosidase improves the accessibility of water to Gd^{3+}, which results in an increase in the relaxivity of the complex (16). The fourth class is the *cell labeling contrast agents*, such as TAT–peptide conjugated iron oxide particles (17) or Gd–HPDO3A (18). In order to meet the diverse requirements sketched above, highly potent, innovative, specific and preferably multimodal contrast agents are required.

Lipid-based colloidal aggregates, such as liposomes, micelles and microemulsions, have been used extensively recent decades as drug carriers to improve pharmacokinetic properties or the bioavailability of the drug, to increase the target-to-background ratio of the drug or to deliver hydrophobic drugs (19–23). The above particles are composed of lipids and/or other amphiphilic molecules. Amphiphiles are molecules with both hydrophobic and hydrophilic parts that spontaneously assemble into aggregates in an aqueous environment. Targeting ligands can be conjugated to the colloidal particles to achieve binding to molecular markers that are specific for disease processes (24,25). Fluorescent labels can easily be incorporated for fluorescence microscopy (26).

A relatively, new applications of nanoparticulate colloids lie in the emerging field of cellular and molecular MR imaging (27,28). Small Gd-based complexes such as Gd–DTPA and Gd–DOTA are widely used as contrast agents for clinical MRI (29). In order to improve pharmacokinetic properties, to introduce target specificity, to make the contrast agent multimodal and, most importantly, to improve the T_1 and T_2 lowering capability, lipidic aggregates containing MRI contrast agents are an attractive option. The aggregate morphology can vary from micelles, through microemulsions to liposomes (30–35).

Colloidal particles in contrast-enhanced MRI have many applications. They can be used as blood pool agents with long circulation times for magnetic resonance angiography (MRA). Another application is the detection of pathological tissues with enhanced vascular permeability, which occurs in inflammation, myocardial infarction, atherosclerosis, breakdown of the blood–brain barrier and tumors. Like lipidic colloids used for drug delivery, the particulate contrast agents can also be conjugated to ligands to target them to a molecular marker of interest, permitting indirect detection of marker distribution by MRI. Furthermore, pH- and temperature-sensitive liposomes can be used to visualize regional differences in these parameters with MRI. For cell labeling purposes, lipidic nanoparticles also hold great promise.

In this review, we will first explain the properties of amphiphilic molecules and their assembly into colloidal aggregates. Different strategies for conjugation of targeting ligands and potential biological targets will be reviewed. The focus of this review is on Gd-containing lipidic nanoparticles and their use for contrast-enhanced and molecular MRI.

AMPHIPHILIC AGGREGATES

Amphiphiles

Amphiphiles, also referred to as surfactants, are molecules that contain both a hydrophobic (non-polar tail) and a hydrophilic (polar head) part [Fig. 1(A), I]. Because of this dual character and the energetically unfavorable contact between the non-polar part and water, amphiphiles self-associate into aggregates of different sizes and geometries. There is a wide variability in both the hydrophobic and hydrophilic parts of amphiphilic molecules. The hydrophobic part can vary in length and can consist of multiple chains, creating different ratios between the size of the hydrophobic and hydrophilic part [Fig. 1(A)]. For the polar headgroup, both the size and charge can vary, dividing these molecules into ionic (anionic or cationic) or non-ionic amphiphiles. These characteristics and parameters such as pH, temperature and concentration, eventually determine the geometry of the aggregate that is formed in aqueous solution. Phospholipids and cholesterol [Fig. 1(A)] are naturally occurring amphiphilic molecules that are important structural

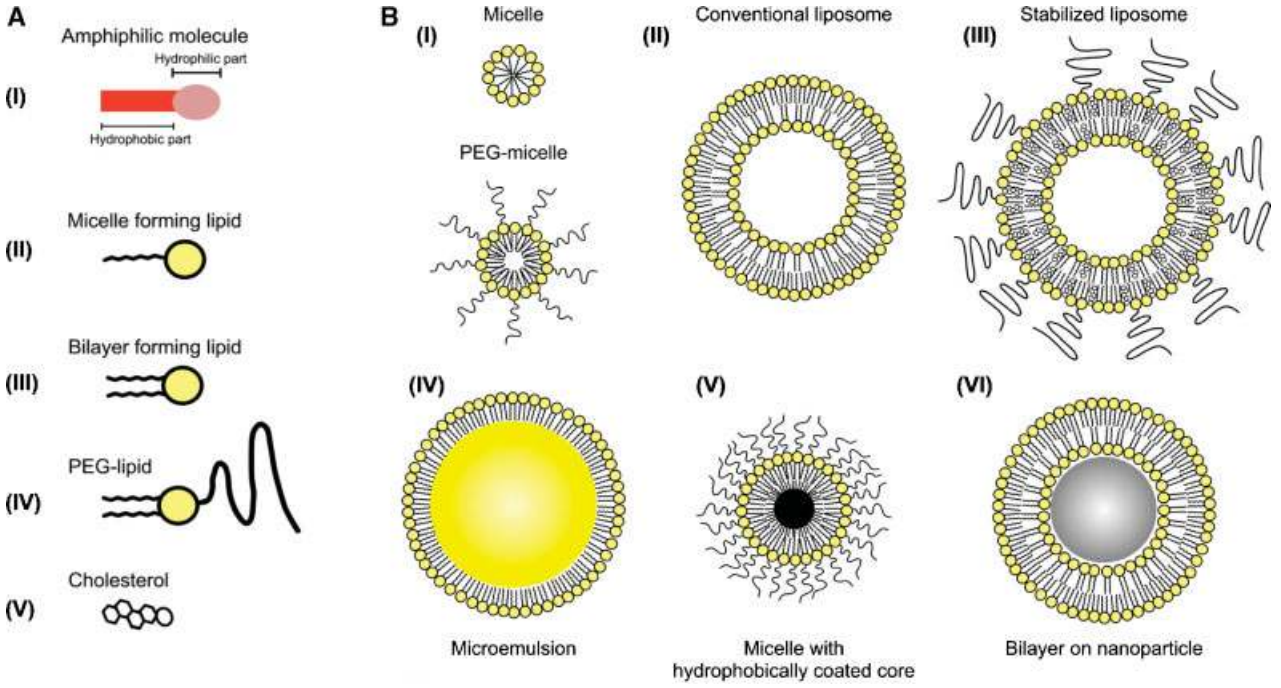

Figure 1. (A) Schematic representation of amphiphilic lipids. (I) Amphiphiles consist of a hydrophilic head and a hydrophobic tail. (II) Micelle-forming lipids have a relatively large head compared with the hydrophobic part, whereas (III) bilayer-forming lipids usually have two hydrophobic tails. (IV) PEG–lipids are used to improve pharmacokinetic properties and (V) cholesterol is used to stabilize liposomes. (B) Possible lipid aggregates for *in vivo* use. (I) Micelles can be prepared from micelles forming lipids and from PEG–lipids. (II) A conventional liposome consists of a phospholipid bilayer. (III) Improved stabilization of liposomes can be achieved by incorporating a small amount of PEG–lipids and cholesterol. (IV) Microemulsions consist of a surfactant (amphiphile) monolayer covering oil. (V) Micelles can contain a hydrophobic nanoparticle. (VI) Bilayer on nanoparticles of silica, mica, glass or iron oxide

elements of biological membranes. In recent years, many phospholipid-like structures have been synthesized to benefit from the amphiphilic character and used to achieve a wide variety of aggregates.

Amphiphile aggregation

The major forces that direct the self-assembly of amphiphilic molecules into well-defined structures in water derive from the hydrophobic associative interactions of the tails and the repulsive interactions between the hydrophilic headgroups (36,37). In these aggregates, the amphiphiles are organized in such a way that the hydrophobic parts cluster together and the hydrophilic headgroups face the water. The length of the hydrophobic chain(s) and the size of the headgroup in relation to the chain determine the curvature of the aggregate and whether a micelle-like structure or a bilayer-like structure will be formed. A wide variety of structures are possible. In the low concentration range, spherical micelles, cylindrical micelles and bilayered vesicles are among the aggregates formed. At higher concentrations, cubic, lamellar and hexagonal phases may occur (36). Furthermore, microemulsions can be formed from water, oil and an amphiphile. These are stable isotropic dispersions of oil covered by a lipid monolayer (38). Another class of lipid aggregates is self-assemblies of lipid mono- or bilayers that contain a solid core. Hydrophobic nanoparticles such as iron oxide (35) and quantum dots (39) can be entrapped in a micellular shell of PEG–lipids, while glass, silica and mica, but also iron oxide nanoparticles (40), can be covered by a lipid bilayer [Fig. 1(B), VI].

For *in vivo* applications, the amphiphilic aggregates should be (i) stable and (ii) biocompatible and (iii) have excellent pharmacokinetic properties. Possible structures for *in vivo* use are depicted in Fig. 1(B). In the case of micelles the hydrophobic part of the amphiphilic molecules forms the core of the micelle and the hydrophilic part forms the micelle corona. Micelles can be formed from lipids with a relatively large headgroup, such as lipids with a single fatty acyl chain [Fig. 1(B), I]. Furthermore, phospholipid mixtures with a high proportion of PEG–lipid will assemble into micelles, owing to steric hindrance of the PEG–lipid headgroups (41). Liposomes are created from bilayer-forming lipids, which are usually comprised of a polar headgroup and two fatty acyl chains [Fig. 1(B), II]. The hydrophobic part of these lipids occupies more space than that of micelle-forming lipids and therefore bilayer formation is energetically favorable. For stabilization of the lipid bilayer, cholesterol is often included (42). In addition, PEG–lipids (3–7%) may be incorporated in the bilayer [Fig. 1(B), III] to increase circulation half-lives *in vivo* and to reduce

interactions of the liposomes with plasma proteins (42). Microemulsions or hydrophobically coated nanoparticles (e.g. iron oxide particles or quantum dots) in micelles are also under investigation for *in vivo* use.

Drug targeting/delivery

Liposomes have been studied extensively to improve the pharmacokinetic properties of mainly water-soluble drugs, while micelles and microemulsions may be used to deliver drugs with poor water solubility (43–47). This has resulted in the approval of several liposomal drug formulations (48,49), which have proven especially successful in tumor targeting (50). Doxorubicin is the most commonly used anticancer agent in liposomal formulations (51). Encapsulating this drug in liposomes has led to improved delivery to the tumor and a reduced exposure of other tissues. Cisplatin, another drug which is used in the treatment of solid tumors, has also been encapsulated in liposomal formulations. Liposomal cisplatin has not been shown to be very effective thus far (52), which is partly ascribed to the low water solubility of cisplatin that causes a low encapsulation efficiency. Recently, a novel lipid formulation with an improved cisplatin-to-lipid ratio and improved cytotoxicity has been described (53).

Accumulation of liposomes at the desired site can be improved by prolonging the circulation time. Conventional liposomes are rapidly eliminated from the circulation by cells of the reticulo-endothelial system in the liver. The clearance rate is enormously decreased when liposomal systems are coated with a hydrophilic polymer such as PEG (54,55), which results in improved bioavailability (56).

Many drugs are poorly water soluble, which results in a low bioavailability. Micelles are currently under investigation as carrier vehicles of such hydrophobic drugs (57,58). Micelles solubilize these drugs by incorporating them into their hydrophobic core and thus increase the bioavailability. Microemulsions have also been investigated for their potential to serve as a drug carrier vehicle. They are interesting, since the oil phase can contain a high payload of hydrophobic drugs (38,59).

Specificity for the desired target tissue or cells can be obtained by conjugating the systems portrayed above with ligands such as antibodies, antibody fragments and peptides (58,60–62). Conjugation strategies and (potential) targets are described in the following sections.

CONJUGATION STRATEGIES

In this part, conjugation strategies will briefly be highlighted. For more in-depth information we refer to excellent reviews describing different conjugation methods (63–65).

There are two main options for the conjugation of a targeting ligand to lipidic particles: non-covalent linkage, such as the avidin–biotin interaction, or covalent binding. Less frequently used methods are the incorporation of amphiphilic targeting proteins in the lipid bilayer of liposomes (66) or the use of amhiphiles with a functional moiety, such as a peptide (67) or a peptidomimetic (68,69).

Lipidic nanoparticles can be prepared containing a wide variety of functionalized lipids. For that purpose, phosphatidylethanolamine (PE) with the functional moiety attached to the phosphate group via a spacer is often used. The spacer can vary in length and lipids containing a PEG spacer with a distal functional moiety are also available. Among the functional groups are biotin, maleimide, PDP, carboxylic acid and amine. Via these functional groups, several targeting ligands, such as mAb, Fab, proteins and peptides, can be conjugated using different coupling strategies. Two popular coupling methods will be explained in more detail.

Avidin-biotin linkage

The avidin–biotin linkage is typified by its elegance and simplicity. Avidin, a tetrameric protein with a molecular weight of 68 kDa, is capable of strongly binding four biotins ($K_A \approx 1.7 \times 10^{15}\,M^{-1}$). The biotin–avidin interaction has been exploited for conjugating liposomes with biotinylated proteins. This strategy has also been used to link MR contrast agents to antibodies (15,70–72). This conjugation method is depicted schematically in Fig. 2(B). A lipidic nanoparticle carrying a lipid with a distal biotin is first incubated with avidin. In a second step, the particle–avidin conjugate is incubated with a biotinylated ligand, e.g. a peptide or antibody. Although this method is simple and effective, the introduction of avidin into the conjugate has certain drawbacks. First, the size of avidin will considerably increase the size of the conjugate. More importantly, avidin is known (73) to be immunogenic and to be rapidly cleared by the liver. In fact, this property of avidin has been exploited to chase and clear antibodies (74) and MRI contrast agents from the circulation (8). Covalently linking the ligand to the lipidic particle directly would lead to a smaller conjugate, which has more favorable pharmacokinetic properties.

Covalent binding

Covalent conjugation of ligands to a lipidic particle can be achieved with several methods. Roughly, these methods can be divided in the formation of (i) an amide bond, between activated carboxyl groups and amino groups, (ii) a disulfide bond and (iii) a thioether bond, between maleimide and thiol. The last approach will be discussed in more detail [Fig. 2(C)], since it is broadly applicable.

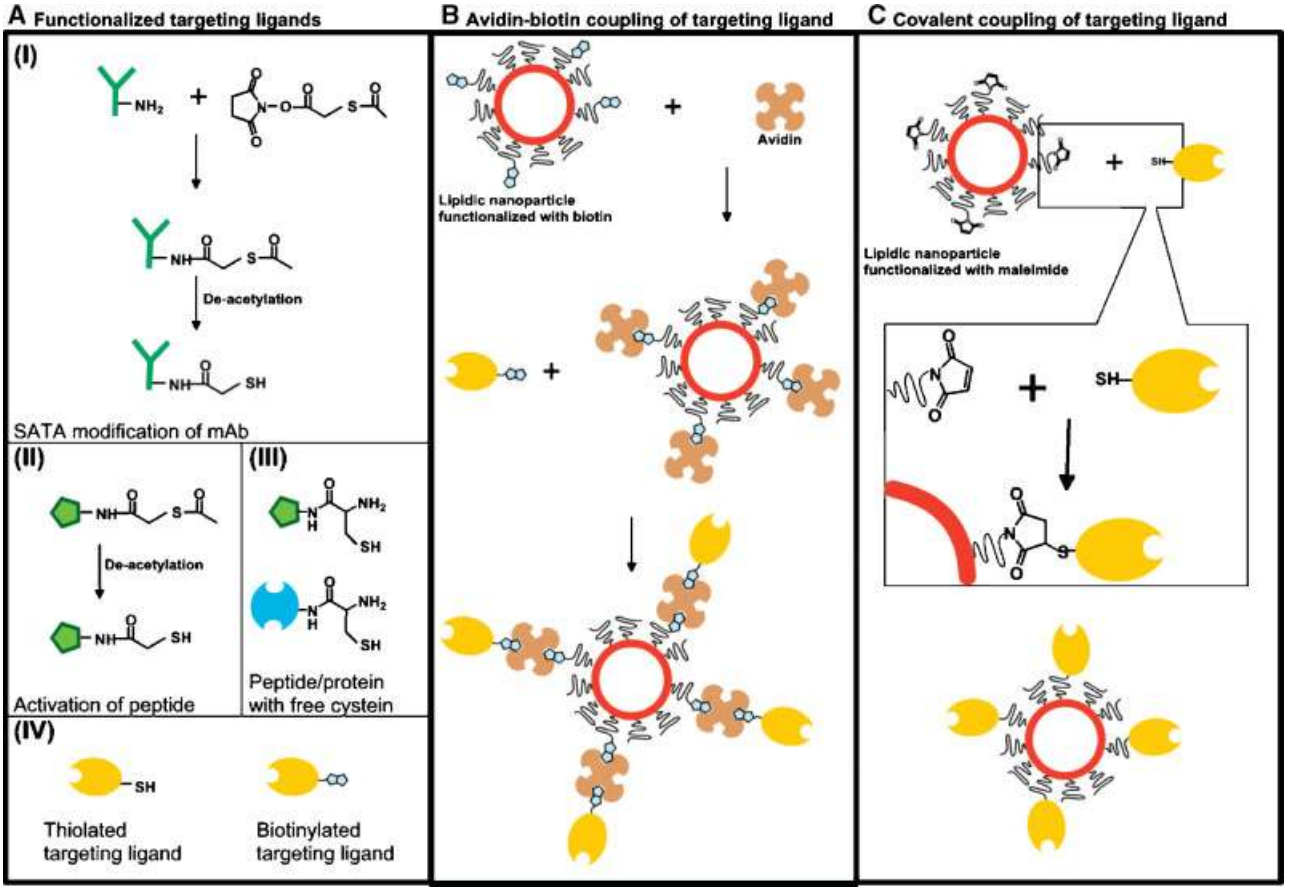

Figure 2. (A) Introducing thiol groups in (I) proteins or antibodies and (II) peptides. (III) Protein and peptide with free cystein. (IV) Targeting ligands with a functional group, i.e. thiol or biotin. (B) Schematic representation of avidin–biotin linkage of a ligand to a lipidic nanoparticle. (C) Schematic representation of maleimide–thiol linkage of a ligand to a lipidic nanoparticle

First, the ligand should expose a free thiol group, necessary for bond formation. Proteins, antibody (fragments) and peptides exposing a free cysteine can directly be used for coupling to maleimide [Fig. 2(A), III]. Peptides synthesized with a protective terminal thioacetate group can be activated upon deacetylation with hydroxylamine [Fig. 2(A), II]. This results in the conversion of the thioacetate into a thiol group. The same strategy is used for proteins that are activated with succinimidyl-*S*-acetyl thioacetate (SATA) [Fig. 2(A), I]. SATA is coupled to free amino groups present in the protein and with hydroxylamine the thioacetate moiety is converted into a free thiol group. The thiol ligands react with maleimide-containing particles and form a covalent thioether linkage, as depicted schematically in Fig. 2(C).

RELAXIVITY OF MACROMOLECULAR CONTRAST AGENTS

The relaxivity, i.e. the potency to shorten the T_1 and T_2 relaxation times of water, of an MRI contrast agent is defined by the change in longitudinal or transversal relaxation rates per unit concentration of the contrast agent (2,3). The constant of proportionality is called the relaxivity, r_1 or r_2, and is expressed in $mM^{-1}\,s^{-1}$. Furthermore, the ratio between r_2 and r_1 determines whether a contrast agent is suitable for contrast-enhanced T_1-weighted imaging or whether it can better be used for contrast-enhanced T_2- and T_2*-weighted imaging. The so-called T_1 agents, typically chelates of Gd^{3+} ions, have a low ratio of r_2 to r_1 (usually between 1.1 and 2) and generate positive contrast (bright/hot spots in T_1-weighted MRI), whereas the T_2 agents have a large r_2 and generate negative contrast (dark/cold spots in T_2- and T_2*-weighted MRI).

The relaxivity of paramagnetic Gd^{3+} chelates is determined by the complex interplay of many parameters governing the dipolar interactions between water and the paramagnetic Gd entity. A complete treatment would be beyond the scope of this review and we therefore restrict ourselves to a qualitative description of some common observations. The most important parameters for understanding the relaxivity of macromolecular contrast agents are the exchange rate τ_m, the coordination number and the rotational correlation time τ_r. The coordination number and the exchange rate τ_m determine the amount of water molecules that can effectively coordinate with

Gd^{3+} and thereby increase the relaxation rate. The rotational correlation time τ_r is important because the lower tumbling rates of macromolecules are responsible for the increase in r_1 that is observed in a typical range of field strengths. A useful way to gain insight into the relaxation behavior of macromolecular contrast agents is to record the r_1 relaxivity as function of frequency, so-called nuclear magnetic relaxation dispersion (NMRD). The NMRD profile of a macromolecular contrast agent shows a typical peak at higher frequencies, in agreement with the increase in the rotational correlation times as compared with low-molecular weight Gd^{3+} chelates. Lipid-based contrast agents can be considered macromolecular contrast agents and the tumbling rate of the Gd chelates in such structures is strongly decreased. As an example, Fig. 3 shows the NMRD profiles of Gd–DTPA and a typical Gd-based liposomal and micellular contrast agent. The NMRD profiles of the liposomes and micelles display the typical peak at higher frequencies. This means that at the clinically relevant field strengths these contrast agents have the highest ionic relaxivity. Furthermore, the amount of Gd chelates per particle is high (varying from 50 for small micelles to several hundred thousand for liposomes). This enhances the relaxivity per contrast agent particle enormously.

T_2 contrast agents usually are superparamagnetic iron oxide particles. The magnetic moments of such particles are much larger than that of Gd^{3+}-containing chelates, typically up to more than three orders of magnitude depending on their size. As a consequence, superparamagnetic particles have a substantially larger r_2 relaxivity compared with paramagnetic contrast agents. The origin of this enhanced relaxivity lies in the strong local field gradients surrounding the superparamagnetic particles, which give rise to accelerated loss of phase coherence of the surrounding water proton spins (4). Increased relaxivity can be observed at a considerable distance from the nanoparticle since, in contrast to the dipolar relaxation, this susceptibility-induced relaxation does not depend on a direct physical contact between protons and the paramagnetic entity.

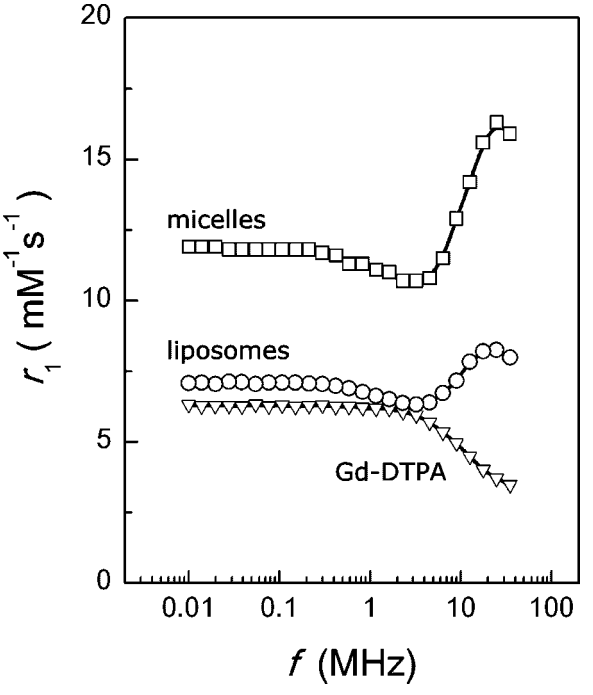

Figure 3. NMRD profiles of Gd–DTPA- and Gd–DTPA-BSA containing liposomes and micelles

For a more quantitative insight into the relaxation characteristics of different lipidic contrast agents described in the literature we have compiled a selection of reported values of r_1 and/or r_2 (Table 1). Direct comparisons between different agents are difficult because of different field strengths and temperatures used. Therefore, we have given the relaxivity of Gd–DTPA measured under the same conditions as a reference. In some studies Gd–DTPA was not measured as a reference. As a reference relaxivity for these contrast agents, the value of Gd–DTPA at 298 K as presented by Aime *et al.* (3) is given. In cases where only an NMRD profile was available for a given contrast agent, we report the relaxivity at 20 and 60 MHz. Furthermore, it should be taken into consideration that the relaxivity is expressed as function of the Gd concentration. The relaxivity per particle is much higher, since the particles depicted in the table carry high payloads of Gd or Fe.

BIOLOGICAL TARGETS

In this section, a number of pathologies will be briefly discussed for which MRI and state-of-the-art contrast agents can be used to image *in vivo* the infiltration of cells and the expression of biological markers to improve the diagnosis of disease and to develop therapeutic strategies.

Inflammation

Inflammation is the body's response to damage, infection, allergy or chemical irritation. Many disorders are associated with inflammation. Inflammation is causative and symptomatic in the destruction of cartilage in rheumatoid arthritis, type I diabetes and loss of intestinal function in Crohn's disease. Inflammatory responses are also observed in cancer, which is accompanied by the massive recruitment of leukocytes in growing tumors (75). In cardiovascular diseases such as myocardial infarction and atherosclerosis, chronic inflammation is causally related to the pathology (76,77). Furthermore, multiple sclerosis, ischemia-reperfusion injury after cerebral stroke and Alzheimer's disease are caused by or associated with inflammatory processes (78).

The inflammatory response involves the migration of leukocytes, the cells of the immune system such as neutrophils, monocytes/macrophages and lymphocytes, into damaged or infected tissues. Recruitment of leukocytes is

Table 1. Overview of the relaxivities of several different lipidic nanoparticulate MRI contrast agents[a]

Aggregate type	Reference	Description	Field strength	Temperature (K)	r_1 Gd–DTPA[b]	r_1[b]	r_2[b]
Liposomes	Tilcock *et al.* (112)	Gd–DTPA in lumen liposomes 400 nm	1.5 T		2.79	0.42	
		Gd–DTPA in lumen liposomes 70 nm	1.5 T		2.79	1.60	
	Kim *et al.* (130)	MHE–DTTA in bilayer liposomes	0.47 T		4.1	31.9	
		BME–DTTA in bilayer liposomes	0.47 T		4.1	27.1	
	Tilcock *et al.* (132)	Stearyl ester–DTPA–Gd in bilayer liposomes	20 MHz[c]	308		23	
		Stearylamide–DTPA–Gd in bilayer liposomes	20 MHz[c]	308		13	
	Storrs *et al.* (30)	Polymerized liposomes long spacer	2.0 T		4.24	12.2	
		Polymerized liposomes short spacer	2.0 T		4.24	5.7	
	Glogard *et al.* (34)	Amphiphilic Gd chelates in bilayer	20 MHz[c]	300	4[d]	47	
		Amphiphilic Gd chelates in bilayer	60 MHz[c]	300	4.5[d]	25	
	Bulte and De Cuyper (40)	Magnetoliposomes	1.5 T	310		3	210
		Stealth magnetoliposomes	1.5 T	310		3	240
	Bertini *et al.* (137)	Paramagnetic liposomes	20 MHz[c]	298	4[d]	12	
		Paramagnetic liposomes	60 MHz[c]	298	4.5[d]	12.5	
	Strijkers *et al.* (149)	Gd–DTPA–BSA-containing liposomes	20 MHz	310	3.8	8.2	
Micelles	Nicolle *et al.* (193)	Gadofluorine	20 MHz[c]	298	4[d]	22	
		Gadofluorine	60 MHz[c]	298	4.5[d]	12	
	Hovland *et al.* (135)	Amphiphilic GdPCTA-[12]	20 MHz[c]	298	4[d]	26	
			60 MHz[c]	298	4.5[d]	28	
	Accardo *et al.* (156)	Mixed micellar aggregates	20 MHz[c]	298	4[d]	18	
			60 MHz[c]	298	4.5[d]	18	
	Mulder and van Tilborg	Micellular iron oxide MCIO (unpublished data)	20 MHz[c]	298	4[d]	15	200
Microemulsion	Winter *et al.* (194)	Nanoparticles Gd–DTPA–BOA	1.5 T	313	4.5[d]	17.7	25.3
		Nanoparticles Gd–DTPA–PE	1.5 T	313	4.5[d]	33.7	50
High-density lipoprotein	Frias *et al.* (102)	HDL-like nanoparticles	65 MHz	298	4.5[d]	10.4	

[a]Note that the ionic relaxivity is given. The relaxivity per particle is much higher, since the particles depicted in the table carry high payloads of Gd or Fe.
[b]r_1 Gd–DTPA: T_1 relaxivity of Gd–DTPA expressed in $mM^{-1}\,s^{-1}$. r_1: T_1 relaxivity of the contrast agent referred to expressed in $mM^{-1}\,s^{-1}$. r_2: T_2 relaxivity of the contrast agent referred to expressed in $mM^{-1}\,s^{-1}$.
[c]NMRD profile was given in the reference.
[d]Data from Aime *et al.* (3).

intricately regulated by inflammatory cytokines such as interferon-γ, tumor necrosis factor-α and interleukin-1. In response to these cytokines, endothelial cells overexpress cell surface adhesion molecules, including the selectins (e.g. E-selectin) that are involved in rolling of leukocytes along the vascular wall, immunoglobulin-like adhesion molecules such as intercellular adhesion molecule-1 (ICAM-1) and vascular cell adhesion molecule (VCAM-1) that support firm adhesion and extravasation of leukocytes into the tissue.

Imaging of inflammatory sites can be achieved by making use of several different characteristics of affected tissues. First, the specific overexpression of endothelial adhesion molecules caused by the exposure

to inflammatory cytokines can be used to target contrast agents. Second, because of the enhanced permeability of blood vessels due to an ongoing angiogenic response, injection of a non-specific contrast agent, preferably a long-circulating contrast agent of relatively high molecular weight, may result in the accumulation of the contrast agent at the inflamed site. Furthermore, migration of cells involved in inflammation can be followed after labeling the cells with an appropriate contrast material. This can be achieved *in vivo*, when a contrast agent is taken up by cells (79) (e.g. monocytes) in the circulation or *ex vivo*, when cells are labeled outside the body and subsequently injected (80). Currently, much effort is being put into research on the targeted imaging of cell adhesion molecules involved in inflammation. Targeting of the adhesion molecule may be done with antibodies, proteins, peptides or small molecules conjugated to an MRI contrast agent. Lipid-based contrast agents have been used for all three strategies (31,81).

Angiogenesis

Angiogenesis, the formation of new blood vessels from pre-existing blood vessels, is a sequence of events that is key in many pathological processes (14,82,83). MR contrast agents can contribute to the detection of angiogenic areas and vessels via two strategies. In the first strategy, the permeability of the angiogenic vasculature is determined with dynamic contrast-enhanced MRI. Recently, it has been demonstrated that the use of contrast agents of high molecular weight gives most insight into vasculature permeability in angiogenesis (14). As an example, albumin triply labeled with a fluorescent label, Gd–DTPA and biotin has been used to investigate angiogenesis by measuring vascular permeability with a combination of fluorescence microscopy and contrast-enhanced MRI (8). The rate of clearance of the latter albumin contrast material from the circulation can be manipulated by actively removing it with an avidin chase. Lipid-based contrast agents can be synthesized in a wide range of sizes, useful for probing vascular permeability and with different functional moieties, e.g. a biotinylated lipid for an avidin chase and a fluorescent lipid and therefore would be very suitable for the applications just described. The second strategy is to target contrast agents to markers that are specifically associated with angiogenically activated endothelial cells. Many cell surface receptors are strongly expressed on activated endothelial cells of angiogenic vessels, as compared with resting endothelial cells of blood vessels in non-diseased tissue. These receptors include $\alpha v\beta 3$-and $\beta 1$-integrins, vascular endothelial growth factor receptor (82), CD36 and CD44 (84). Especially the $\alpha v\beta 3$-integrin has been shown to be very useful as a target for therapies and molecular imaging contrast agents. In addition to $\alpha v\beta 3$-specific antibodies, the $\alpha v\beta 3$-specific RGD peptide and peptidomimetics have been used in several studies. The expression of this integrin has been non-invasively visualized in tumor-bearing mice with a combination of radiolabeled RGD and positron emission tomography (85). Gene delivery with $\alpha v\beta 3$-targeted lipidic nanoparticles in tumor-bearing mice resulted in tumor cell apoptosis and sustained regression of the tumors (68).

Apoptosis

Apoptosis, or programmed cell death, is essential for tissue development and homeostasis. Deregulation of the apoptotic program is often found to play a critical role in the etiology of various pathological conditions, including neurodegenerative diseases, autoimmune diseases, cardiovascular diseases, tumor development and organ transplant rejection. In addition, chemotherapeutic drugs or radiation therapy often rely on the induction of apoptotic cell death. Therefore, the *in vivo* detection of apoptosis could be of great importance for the evaluation of disease progression or disease treatment. Several studies have been performed in which the detection of apoptosis was based on the expression of the lipid phosphatidylserine (PS) on the outer layer of the apoptotic cell membrane. The expression of this phospholipid can be detected with annexin V or synaptotagmin I conjugates. Both proteins bind with high affinity to PS in a Ca^{2+}-dependent manner. Koopman *et al.* (86) were the first to describe the use of FITC-conjugated annexin V for the detection of apoptotic B cells with flow cytometry. The first *in vivo* visualization of programmed cell death was carried out with radiolabeled annexin V (87) in various animal models and thereafter in patients with acute myocardial infarction (88). Annexin V, conjugated to fluorescent dyes, has been used for *in vivo* optical imaging in the beating murine heart (89) and recently several Cy5.5-conjugated annexin V probes have been introduced for near-infrared fluorescent imaging (90). Annexin V-functionalized cross-linked iron oxide (CLIO) was designed as a contrast agent for MRI, which was additionally labeled with Cy5.5 to allow co-localization with optical imaging techniques (91). Alternatively, conjugation of multiple Gd–DTPA molecules or superparamagnetic iron oxide particles (SPIO) to the C2 domain of synaptotagmin I was shown to allow the detection of apoptotic cells *in vitro* (92). Zhao *et al.* (93) were the first to apply a C2 domain-functionalized SPIO and showed very promising results for future *in vivo* applications of MR contrast agents for the detection of apoptotic sites.

Tumors

Although the above-described processes of angiogenesis, apoptosis and inflammation are targets themselves in the development of anti-cancer therapies, a lot of research is

currently being performed on the development of targeted therapies directed at tumor cells. Signal transduction research has shown the importance of the human epidermal growth factor receptor (HER) family of transmembrane tyrosine kinases in a number of solid tumor types. One member of this family is HER-2 (ErbB-2), which is overexpressed in several types of cancers, including breast, lung, gastric and bladder carcinomas. HER-2 expression is similar in primary tumors and corresponding metastases (94). The expression in normal tissues is very low, making HER-2 a candidate for targeting strategies. Also, the epidermal growth factor receptor (EGFR, also known as ErbB-1 or HER-1), an important molecule in the proliferation and metastasis of tumor cells, is frequently overexpressed in common solid tumors and has become a favored target for therapy with monoclonal antibodies directed at the extracellular domain of the receptor and for therapy with small molecule inhibitors of the receptor's tyrosine kinase activity (95).

In addition to therapy based on blocking the receptor and thereby achieving inhibition of tumor cell growth and metastatic potential, these receptors can also be used for targeted delivery of drugs or diagnostic imaging agents (96). Targets expressed at tumor cells are more difficult to use for molecular MRI since they cannot be reached directly via the circulation, but require the contrast agent to leak from the blood vessels into the extravascular compartment. Since most molecular MRI contrast agents are nanoparticulate materials, this poses a limit on imaging such extravascular receptors. Nevertheless, molecular MRI of the HER-2/neu receptor, expressed at tumor cells, with avidin–Gd complexes after prelabeling the receptors with biotinylated anti-HER-2/neu antibody has been demonstrated (97). Furthermore, HER-2/neu-targeted immunoliposomes effectively associate with tumor cells and show antitumor efficacy (98).

Atherosclerosis

Atherosclerosis is a progressive disease, which can be considered a chronic inflammation of the large arteries (99,100). The disease starts with inflammation-like endothelial dysfunction caused by local injury or by the retention of atherogenic lipoproteins. The process is initiated by oxidized lipoproteins in the vessel wall, e.g. oxLDL, which triggers the endothelium to express monocyte recruiting endothelial cell receptors such as VCAM-1, P-selectin, E-selectin and ICAM-1. Monocytes accumulate in the subendothelial space and differentiate into macrophages that take up oxLDL. Eventually, the macrophages are converted into foam cells. At this stage of the disease the lesion is called an early lesion or a fatty streak. With continuing lipoprotein accumulation and foam cell formation, the early lesion progresses into an atheromatous core. The atherosclerotic plaque thus formed is stabilized by the migration of smooth muscle cells, resulting in the formation of a fibrous cap. Blood supply into the heavily thickened vessel wall is maintained by an angiogenic expansion of the vasa vasorum (vessels within the wall of larger blood vessels) (101). The advanced plaque, or complex lesion, may be at risk of rupture, which triggers thrombus formation. This process is the main cause of acute clinical complications such as stroke and myocardial infarction.

In this cascade of events, several markers are of interest for target-specific MRI. LDL or HDL can be paramagnetically labeled (102,103) for identification of atherosclerotic plaques after uptake of these contrast agents by the plaque. All inflammatory markers, e.g. E-selectin, P-selectin or VCAM-1, expressed on the endothelial cell are potential targets for molecular MRI of atherosclerosis. Fluorescent and superparamagnetic iron oxide nanoparticles have been successfully targeted to plaques in transgenic mice using a VCAM-1-specific peptide (104). Furthermore, monocytes and other cells related to inflammation can be magnetically labeled, *in vivo* and *ex vivo*, to follow their fate in relation to atherosclerosis. Since strong angiogenic activity may occur in the vasa vasorum, strategies sketched in the section about angiogenesis also have potential in identifying and characterizing atherosclerotic plaques. In advanced stages of plaque formation, apoptotic activity is common and contributes to plaque instability. Detection of apoptotic plaques with MRI would therefore give the opportunity to determine the risk of plaque rupture *in vivo*. Strategies to image apoptosis are outlined in the section on apoptosis. In the final stage of the atherosclerotic progression, thrombi, e.g. formed as a result of plaque rupture, can be targeted with fibrin or platelet-specific peptides (105) or antibodies (72).

LIPID-BASED MRI CONTRAST AGENTS: APPLICATIONS

Liposomal contrast agents

In this section, an overview of liposomal MRI contrast agents is given. A brief outline of historical developments is followed by a summary of what has been done thus far. In the second, part a number of interesting and innovative developments are reviewed and discussed in more depth.

Liposomes were discovered in the early 1960s by Bangham *et al.*, who found that egg lecithin phospholipids combined with water self-organized into spheres because of the amphiphilic character of the lipids (106). Liposomes can be defined as spherical, self-closed structures formed by one or several concentric lipid bilayers with an aqueous phase inside and between the lipid bilayers (107). Liposomes have been used extensively as a model to study the properties of biological membranes. They can vary in size and lamellarity and are therefore subdivided into multilamellar vesicles (MLV), consisting of several concentric bilayers, large

unilamellar vesicles (LUV), in the size range 200–800 nm), and small unilamellar vesicles (SUV), in the size range 50–150 nm. Soon after the discovery of liposomes, they were suggested for use as drug carriers, because of their striking biological properties. First, liposomes are composed of naturally occurring lipids or closely related synthetic lipids and therefore are biocompatible. Liposomes can carry water-soluble pharmaceutical agents in the aqueous interior and amphiphilic or hydrophobic agents in the lipid bilayer. Furthermore, liposomal pharmaceutical agents are protected from interactions with plasma proteins and deactivation and exhibit prolonged circulation times and favorable biodistribution properties. Altering their surface properties makes possible improved delivery of liposomes to diseased tissue and into cells. These properties also make liposomes excellent candidates to carry or deliver contrast agents for MRI and in the 1980s the first studies about the use of liposomes as carriers of MR contrast agents appeared in the literature.

The first type of liposomal MRI contrast agents described were liposomes entrapping paramagnetic agents in the aqueous lumen. Paramagnetic agents such as $MnCl_2$, (108,109) Gd–DTPA (110–112), Mn–DTPA (113), Gd–DTPA–BMA (114) and Gd–HP–DO3A (115) and macromolecular contrast agents such as Mn^{2+} bound to serum proteins (116) can be prepared in a liposomal formulation. Contrast agents of this type have been used successfully to improve the detection of tumors in the liver of rats with hepatic metastases (117–119). Recently, gadodiamide- and doxorubicin-containing liposomes were used to study the liposomal distribution after convection-enhanced delivery to brain tumors in rats (120) and mice (121). Furthermore, gadobutrol-containing liposomal carriers equipped with RGD ligands were targeted to $\alpha v\beta 3$-integrin-expressing cells *in vitro* (122). Although the liposomal formulations containing a paramagnetic payload in the aqueous lumen have been used successfully, the utility of these contrast agents is limited. First, the relaxivity of the entrapped paramagnetic species is lowered, because of the limited exchange of bulk water with the contrast agents (112,123). This exchange is dependent on the permeability of the liposomal membrane to water (124). The permeability of the liposomal membrane depends on the lipid composition and can be altered by varying the saturation level of the lipid chains and the length of the lipid chains and by incorporation of cholesterol. The more permeable the membrane, the better is the water flux across the bilayer and the better the relaxivity (112). Furthermore, the contrast efficiency can be improved by using smaller liposomes. The volume-to-surface ratio of small liposomes is lower and therefore the exchange with external bulk water is better (112,123). This implies that in terms of relaxation properties, an optimal formation would be liposomes of small size with a permeable bilayer. Unfortunately, permeable liposomes usually are less stable in serum than liposomes with a more rigid bilayer. A second drawback is that upon degradation the liposomes may lose their paramagnetic content, which makes the interpretation of observed contrast enhancement problematic. Nowadays, such systems are still in development and the drawbacks just described have also been used beneficially, e.g. for monitoring drug release from liposomes (125) and to use membrane transition properties to monitor local tissue temperature (126) or pH (127). More about this subject will be discussed in a later section about smart contrast agents.

A second class of liposomal contrast agents carries the paramagnetic molecule in the lipid bilayer, which makes the amphiphilic paramagnetic complexes an integral part of the liposomal surface (128,129). This approach results in an improved ionic relaxivity of the metal compared with the approach of encapsulating the paramagnetic molecules in the aqueous interior and compared with low molecular weight complexes (130). The amphiphiles used can consist of Gd–DTPA as the hydrophilic part attached to a hydrophobic part. DTPA–stearate (131,132) or DTPA attached to alkyl chains via amide linkers are examples of such molecules (133,134). Phosphatidylethanolamine (PE) has been linked to DTPA to obtain PE–DTPA, which can form vesicles when mixed with natural phospholipids (135). The NMRD profiles, field-dependent relaxation measurements, closely resemble those of macromolecular contrast agents, with a typical peak at higher field strengths (34,132), because of the longer rotational correlation time. The applicability of such liposomal contrast agents is broad. Pegylated liposomes have been used as a blood pool agent (136), for the detection of lymph nodes (136) and to achieve sustained contrast enhancement of tumors (137). Regions of enhanced permeability can be detected upon injection of paramagnetic liposomes, which is useful e.g. after myocardial infarction (138) and for tumor detection. Recently, the biodistribution of lipoplexes, cationic liposomes bound to DNA, was evaluated over time by incorporating a Gd–lipid amphiphile (139). Upon intratumor injection of the lipoplexes, a strong and persistent T_1-weighted MRI signal increase was observed.

Polymerized liposomes. In 1995, Storrs *et al.* introduced a novel liposomal MRI contrast agent (30). A DTPA-based lipid, amphiphilic carrier lipids and a biotinylated amphiphile, all containing a diacetylene triple bond in the fatty acyl chains, were synthesized. From these lipids, liposomes were prepared and for further stabilization the triple bond-containing lipids in the liposomes were illuminated with UV radiation to induce polymerization via the triple bonds. The biotin group in these polymerized vesicles was used for conjugation of biotinylated antibodies via an avidin–biotin linking procedure. In rats, the half-life of this contrast agent is almost 20 h (140). Sipkins *et al.* used the vesicles coupled

to $\alpha v\beta 3$-specific LM609 antibodies to detect angiogenesis in tumor-bearing rabbits (15). Since MRI has an inherently low sensitivity compared with nuclear methods, the detection of the expression of sparse epitopes should be done with a powerful targeted contrast agent. The polymerized liposomes used in this study were 300–350 nm in size and contained 30% of the Gd–lipid. This means that these liposomes have an extremely high payload of gadolinium per particle, which makes them very potent. The contrast agent was applied intravenously in tumor-bearing rabbits, which resulted in a statistically significant signal intensity enhancement 24 h after injection. Importantly, the signal enhancement correlated with the immunohistochemical determination of $\alpha v\beta 3$-integrin distribution. In later studies, this polymerized liposomal system, targeted to the $\alpha v\beta 3$-integrin, was used to deliver a mutant Raf gene (ATPmu-Raf) to angiogenic blood vessels in tumor-bearing mice (68). ATPmu-Raf blocks endothelial signaling and angiogenesis in response to multiple growth factors. Apoptosis of the tumor-associated endothelium was induced by systemic injection of the liposomes into mice, which resulted in sustained regression of the tumors.

The above liposomal system was also used to detect the expression of leukocyte adhesion molecules with MRI in the brain of mice with experimental autoimmune encephalitis (EAE) (71), a mouse model of multiple sclerosis. To that end, the polymerized liposomes were conjugated to biotinylated antibodies specific for ICAM-1. Mice were injected with ICAM-1-specific liposomes and non-specific liposomes. The brains of the animals were removed and scanned *ex vivo* with high-resolution MRI. Marked differences were observed between EAE mice that were injected with the specific contrast agent and the control contrast agent and healthy mice that were injected with the specific contrast agent (Fig. 4). T_1-weighted images of the EAE mice that had received ICAM-1 specific liposomes demonstrated widespread MR signal intensity increases throughout the central nervous system, which correlated with the pattern of ICAM-1 expression as determined immunohistochemically.

Magnetoliposomes. Magnetoliposomes are liposomes containing solid iron oxide particles in the liposomal lumen (40). Magnetoliposomes have been used originally to study biological membranes (141) and for cell sorting (142). Furthermore, they can be used for targeted drug delivery (using a constant magnetic field) and controlled release (using high-frequency magnetic field oscillations) of an entrapped drug (143,144). Two types of magnetoliposomes have been used most often. The first type contains water-soluble iron oxide particles in the aqueous lumen (145,146). The second type, developed by De Cuyper and Joniau, (147), is an iron oxide particle of $\sim$15 nm covered with a lipid bilayer. The latter will be discussed in more detail, since it has been applied as an MRI contrast agent *in vivo*. The formation of this type of magnetoliposome starts with the synthesis of a magnetic fluid of superparamagnetic iron oxide particles. The iron oxide particles are stabilized and solubilized with laurate. When the particles are incubated with an excess of phospholipid vesicles and dialyzed for a number of days, the phospholipids from the vesicles transfer and absorb on the solid surface, ultimately forming a bilayer of phospholipids around the iron oxide particles. For improved pharmacokinetic properties, PEG–lipids can be introduced by simply mixing the magnetoliposomes with donor vesicles containing these lipids. The PEG–lipids transfer spontaneously from the donor membranes to the bilayer of the magnetoliposomes. Bulte *et al.* demonstrated the applicability of this nanoparticle as a bone marrow MR contrast agent (148). Furthermore, the pegylated magnetoliposomes can be functionalized through incorporation of a PEG–lipid with a distal functional moiety, which can be used for conjugation to achieve specificity for the biological marker of interest.

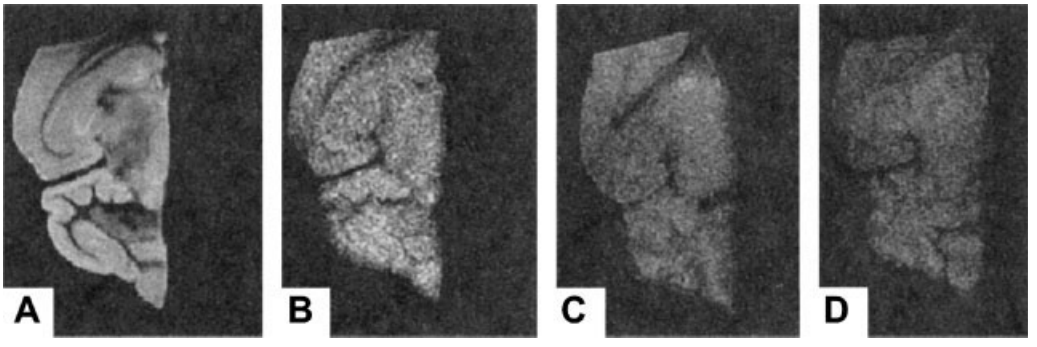

Figure 4. High-resolution MR images of the EAE mouse brain with anti-ICAM-1 PV contrast enhancement vs controls. (A) T_2-weighted MR image of *ex vivo* EAE mouse brain. T_1-weighted MR image of *ex vivo* mouse brain (B) with and (D) without EAE after injection of anti-ICAM-1 antibody-conjugated paramagnetic liposomes. (C) EAE mouse brain after injection of control isotype antibody-conjugated paramagnetic liposomes. Widespread MR signal intensity enhancement throughout the brain with EAE can be observed for (B) only. Adapted from Fig. 4 of Sipkins *et al.*, ICAM-1 expression in autoimmune encephalitis visualized using magnetic resonance imaging. *J. Neuroimmunol.* 2000; **104**: 1–9, with permission from Elsevier Science

Bimodal liposomes. Mulder *et al.* introduced a bimodal targeted liposomal contrast agent for the detection of molecular markers with both MRI and fluorescence microscopy (31,149). The liposomes consist of Gd–DTPA attached to two stearyl chains, a fluorescent lipid, DSPC, cholesterol and PEG–DSPE. The last component provides the liposomes with a hydrophilic coating for improved stability *in vivo*. *In vitro*, this contrast agent conjugated with E-selectin-specific antibodies was tested on human endothelial cells (HUVEC) stimulated with tumor necrosis factor α (TNFα). A pronounced contrast agent association was observed with fluorescence microscopy at the subcellular level and with MRI on cell pellets (31).

Furthermore, apoptotic jurkat cells were successfully targeted and imaged *in vitro* with the bimodal liposomal contrast agent conjugated with Annexin-V (150). Following incubation with the contrast agent, pellets of apoptotic cells showed increased signals in T_1-weighted images, whereas it was revealed with confocal laser scanning fluorescence microscopy that the contrast agent was bound to the cell surface.

The liposomal contrast agent conjugated with cyclic RGD–peptides was used to identify the angiogenic endothelium in tumor bearing mice with *in vivo* MRI and *ex vivo* fluorescence microscopy (151,152). The cyclic RGD–peptide has high affinity for the $\alpha v\beta 3$-integrin, which is upregulated at endothelial cells of angiogenic blood vessels. MRI revealed that upon intravenous injection of the contrast agent, the RGD–liposomes localized to a large extent in the tumor rim, which is known to have the highest angiogenic activity [Fig. 5(A)]. Non-specific RAD-liposomes also targeted the tumor, but showed a diffuse distribution pattern [Fig. 5(B)]. The different mechanisms of accumulation were established with fluorescence microscopy, which revealed that RGD–LNP were exclusively associated with tumor blood vessels [Fig. 5(C)] whereas RAD–LNP were, to a large extent, localized in the extravascular compartment [Fig. 5(D)]. This study demonstrated the critical importance of validating the MRI findings with a complementary technique such as fluorescence microscopy.

Micellular contrast agents

Micelles are in particular interesting for carrying poorly soluble pharmaceutical agents (153). Furthermore, they

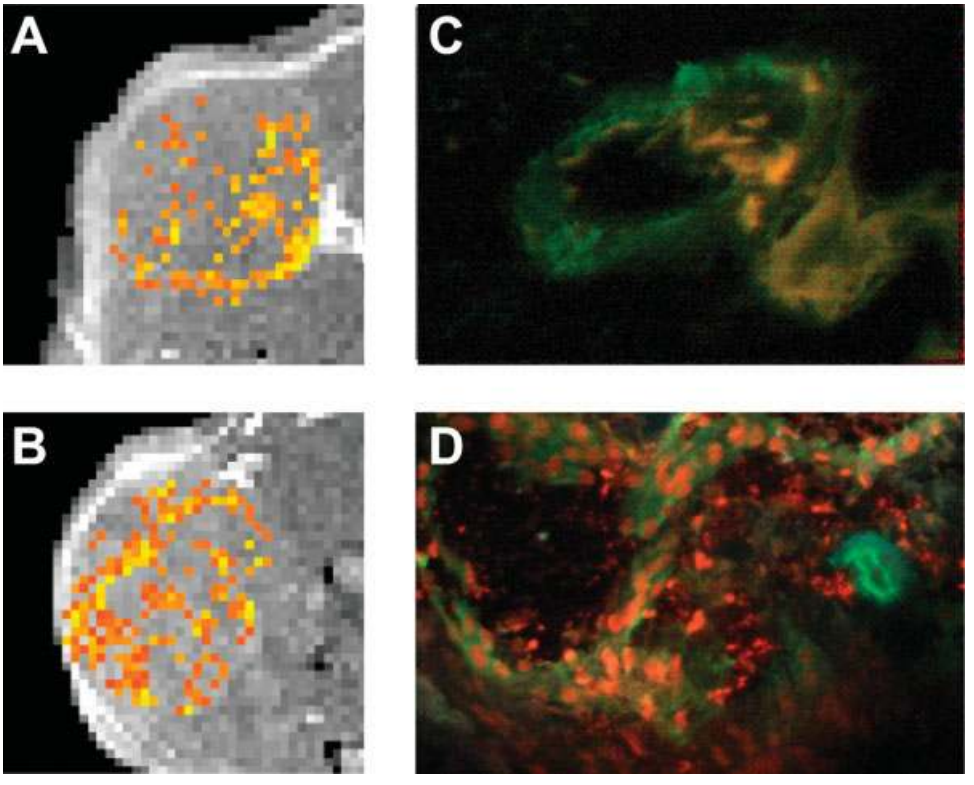

Figure 5. MR images of tumors of mice after they were injected with (A) paramagnetic $\alpha v\beta 3$-specific RGD–liposomes and (B) non-specific paramagnetic RAD–liposomes. Fluorescence microscopy of 10 μm sections from dissected tumors revealed a distinct difference between tumors of mice that were injected with RGD–liposomes (C) or RAD–liposomes (D). Vessel staining was done with an endothelial cell-specific FITC–CD31 antibody. The red fluorescence represents the liposomes (C) and the green fluorescence represents blood vessels. RGD–liposomes were exclusively found within the vessel lumen or associated with vessel endothelial cells (C), whereas RAD–liposomes (D) were also found outside blood vessels within the tumor

can be prepared from lipids that contain a PEG moiety to make the surface of the micelle inert to blood components. This lets micelles circulate in the blood for a fairly long time without being recognized by certain plasma proteins and/or phagocytic cells. In this way, they can be used as long-circulating blood pool agents, which non-specifically target to areas with a leaky vasculature. Ligands can also be coupled to the surface of the micelles for targeting to specific sites (154). These properties make micelles excellent candidates to function as MRI contrast agents. The most common strategy to prepare micelles with paramagnetic properties is to use amphiphilic molecules with a Gd^{3+} chelating and hydrophilic headgroup and one hydrophobic chain. A mixture of paramagnetic amphiphilic molecules and phospholipids or PEG–lipids may also be employed. The NMRD profile of a micellular contrast agent shows the typical peak in the T_1 relaxivity r_1 at higher field strengths (155), since micelles have a relatively long rotational correlation time, typical for macromolecular contrast agents. The ionic relaxivity of Gd-based micellular contrast agents at clinically relevant field strengths is therefore superior to that of low molecular weight complexes. Recently, Accardo *et al.* described the synthesis and physiochemical characterization of a target-specific micellular contrast agent which was composed of a mixture of two amphiphilic molecules (156). The first molecule is a C_{18} hydrophobic moiety bound to an octapeptide. The second molecule contains the same C_{18} moiety, but is coupled to DTPA. The peptide sequence used displays high affinity for cholecystokinin receptors, which are localized in the cell membrane and overexpressed in many tumors. The authors inferred that this type of mixed micellular contrast agent is a promising tool for target-specific MR imaging.

Micelles composed of phospholipids, a surfactant and an amphiphilic Gd contrast agent were recently used for detecting macrophages (157). Macrophages are known to play a central role in the pathogenesis and evolution of atherosclerotic plaques. The contrast agent was employed to macrophages *in vitro* and *in vivo* in a mouse model of atherosclerosis and showed macrophage-specific uptake. Immunomicelles were prepared by coupling biotinylated antibodies, specific for the macrophage scavenger receptor, to the micelles via an avidin–biotin linkage. An improved uptake of the antibody conjugated micelles compared with bare micelles was observed, which was established with MRI and fluorescence microscopy.

Gadofluorine. Gadofluorine is a micellular contrast agent composed of a surfactant with a highly hydrophobic perfluoroalkyl tail and a hydrophilic Gd^{3+} chelating headgroup and has been shown to be especially successful for MR lymphography (158–160) and improved detection of atherosclerotic plaques (81,161). Barkenhausen *et al.* studied the aortic arch of hyperlipidemic rabbits with MRI before and after the administration of gadofluorine

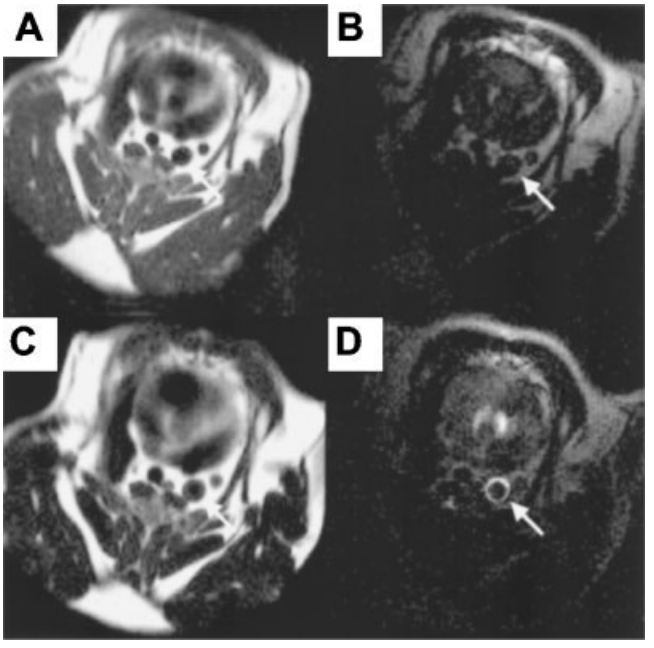

Figure 6. HASTE (A, C) and IR turboFLASH (B, D) images before (A, B) and 48 h after (C, D) application of gadofluorine to an 18-month-old WHHL rabbit at identical slice positions. Wall of descending aorta (arrows) shows marked enhancement after contrast injection (D). Adapted from Fig. 2 of Barkhausen *et al.*, Detection of atherosclerotic plaque with gadofluorine-enhanced magnetic resonance imaging. *Circulation* 2003; **108**: 605–609, with permission from Lippincott Williams & Wilkins

(81). Enhancement occurred in the aortic wall of all hyperlipidemic rabbits. In Fig. 6, images before (A and B) and 48 h after (C and D) application of the contrast agent are depicted. A ring-shaped contrast enhancement of the aortic wall was observed. The MRI findings were validated with Sudan Red staining and matched with *ex vivo* MR scans of the same specimen. Sirol *et al.* demonstrated that gadofluorine is especially useful for detecting lipid-rich plaques (162). Furthermore, using an improved scanning protocol the authors were able to detect atherosclerotic plaque within 1 h after gadofluorine injection. Another study by Sirol *et al.* demonstrated that early and advanced lesions can be discriminated by gadofluorine-enhanced imaging (163). Upon injection of gadofluorine, early lesions showed lower enhancement than more advanced lesions. This correlated with the density of the vasa vasorum, suggesting that plaque enhancement with gadofluorine is dependent on neovessel density. Gadofluorine has also been shown to be useful for the assessment of nerve degeneration, since it selectively accumulated and retained in nerve fibers undergoing Wallerian degeneration in the leg of rats causing bright contrast on T_1-weighted MR images (164).

Nanoparticle-containing micelles. Nanoparticles, such as iron oxide particles and quantum dots, are mostly synthesized in non-polar organic solvents and capped

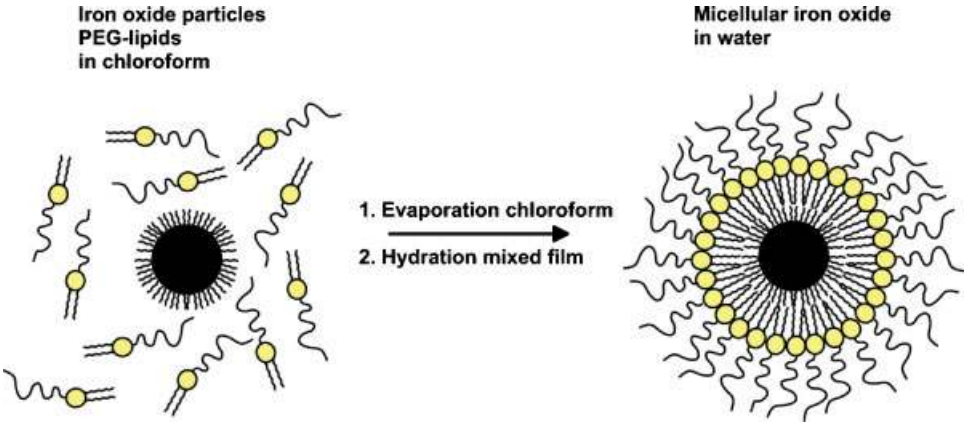

Figure 7. Schematic representation of the encapsulating procedure of hydrophobic nanoparticles in micelles. Lipids are mixed with the nanoparticles in an apolar solvent. The mixed film obtained is hydrated. Thereafter, the nanoparticle-containing micelles and empty micelles are separated by centrifugation

with a surfactant. If they are to be solubilized in aqueous buffers, their hydrophobic surface components must be replaced by amphiphilic ones. An alternative strategy was developed by Dubertret *et al.* for TOPO-coated quantum dots (39). The hydrophobic particles were dissolved in chloroform together with pegylated phospholipids. After evaporating the solvent and hydrating the mixed film of quantum dots and lipids, quantum dot-containing micelles were formed. The same method can be used for encapsulating hydrophobic iron oxide particles in micelles. With this elegantly simple procedure, one obtains a water-soluble particle of small size, which can easily be functionalized by just mixing the appropriate lipids. Furthermore, fluorescent lipids can also be incorporated for optical imaging. In Fig. 7, the procedure is described schematically. Van Tilborg *et al.* functionalized the micellular iron oxide particles with Annexin V for the detection of apoptotic cells. *In vitro*, the Annexin V-conjugated particles showed a high affinity for apoptotic cells, which resulted in a large decrease in T_2 of a pellet of these cells, whereas the control cells showed almost no T_2 decrease (165). *In vivo*, this contrast agent might be very useful for detecting apoptotic cells in pathological processes such as ischemic reperfusion injury, atherosclerosis and tumors. Nitin *et al.* developed a similar approach to solubilize iron oxide (35). They conjugated TAT–peptides and a fluorescent label to the distal end of the PEG chains of the phospholipids to coat the iron oxide particles. The TAT–peptide has been shown to deliver nanoparticles into cells, making it attractive for intracellular labeling. The uptake of this conjugate was demonstrated *in vitro* with both MRI and fluorescence microscopy.

Microemulsions

Microemulsions are mixtures of water, oil and an amphiphile, which result in an optically isotropic and thermodynamically stable solution (38). The usefulness of microemulsions as MRI contrast agent was recognized by Lanza and Wickline. Their nanoparticle has a perfluorocarbon core, which is covered with a monolayer of lipids. Initially they used their technology in combination with ultrasound, because of the acoustic properties of the contrast agent. In their first study, a three-step approach to target thrombus was utilized (166). First a biotinylated antifibrin monoclonal antibody was used to target fibrin, a main component of thrombus. Next, avidin was administered to bind to the antifibrin antibodies via a biotin–avidin linkage. Since avidin has four binding sites for biotin the non-bound sites of avidin could next be used for targeting the biotinylated perfluorocarbon nanoparticles. In this manner, thrombi were detected with ultrasound. A similar approach was used for detecting fibrin in dogs with MRI (72). With that aim, Lanza *et al.* slightly modified their procedures by also incorporating paramagnetic lipids (Gd–DTPA–BOA) in the lipid monolayer of the nanoparticles. Because of the size of the nanoparticle, the payload of Gd–DTPA–BOA was as high as 50 000 per particle. This dramatically increases the relaxivity per particle, which is necessary for detecting sparse epitopes with MRI. Scanning electron micrographs of control fibrin clots and fibrin clots targeted with the paramagnetic nanoparticles are depicted in Fig. 8(A) and (B). An extensive association of the contrast agent with the clots can be observed. An *in vivo* MR image of a dog with thrombus (in the external jugular vein) after incubation with the contrast agent shows a pronounced contrast enhancement of the thrombus on T_1-weighted images [Fig. 8(C) and (D)]. In a paper published in 2002, these authors extended their technology for simultaneous imaging and delivery of an antiproliferative drug to smooth muscle cells (167). Furthermore, the perfluorocarbon core of the nanoparticles allows particle detection with ^{19}F NMR spectroscopy, which makes quantification of drug delivery possible. Morawski *et al.* used cultures of

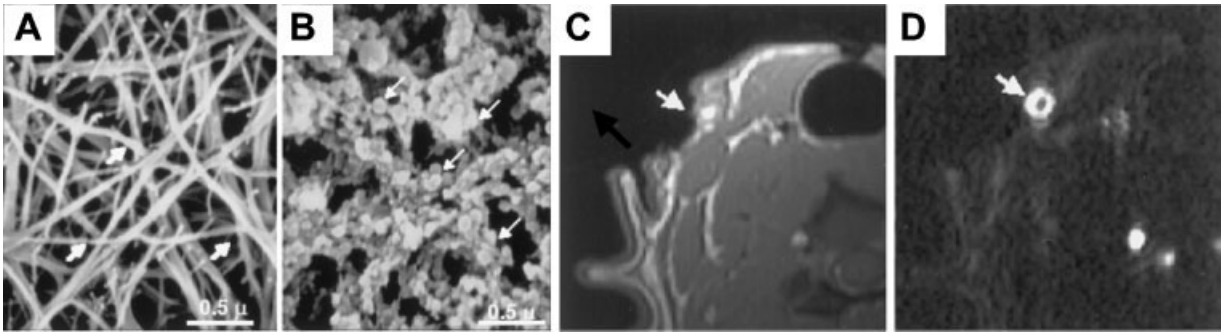

Figure 8. Scanning electron micrographs of control fibrin clot (A) and fibrin-targeted paramagnetic nanoparticles bound to clot surface (B). Arrows indicate (A) fibrin fibril and (B) fibrin-specific nanoparticle-bound fibrin epitopes. Thrombus in external jugular vein targeted with fibrin-specific paramagnetic nanoparticles demonstrating dramatic T_1-weighted contrast enhancement in gradient-echo image (C) with flow deficit (arrow) of thrombus in corresponding phase-contrast image (D). Adapted from Figs 1 and 5 of Flacke *et al.*, Novel MRI contrast agent for molecular imaging of fibrin: implications for detecting vulnerable plaques. *Circulation* 2001; **104**: 1280–1285, with permission from Lippincott Williams & Wilkins

smooth muscle cell monolayers to model and validate the MRI detection limit of sparse molecular epitopes when targeted with this contrast agent (168). They showed that imaging of cell monolayers was possible at 1.5 T using perfluorocarbon nanoparticles of 250 nm, containing 90 000 Gd–DTPA–BOA, targeted to tissue factor-expressing cells. Furthermore, quantification was achieved and picomolar concentrations of the nanoparticles were sufficient to generate a significant change in contrast to noise ratio. The perfluoro nanoparticles targeted to the $\alpha v\beta 3$-integrin have been used for detecting angiogenesis in a rabbit model of atherosclerosis (169) and in tumors implanted in rabbits (69). Angiogenesis plays an important role in providing the tumor with nutrients. Anti-angiogenic therapies are therefore believed to provide a powerful treatment option for cancer. In atherosclerosis the plaques contain angiogenic microvessels, which are believed to play an important role in plaque development. Imaging plaques and tumors with an $\alpha v\beta 3$-specific contrast agent is therefore of importance for early detection, defining the severity of the disease and following the effect of therapy. Recently, Winter *et al.* presented results of a combinatory approach of MR molecular imaging and drug targeting of atherosclerosis with this contrast agent (170). To that end they used the $\alpha v\beta 3$-specific nanoparticles to target the aortic vessel wall after balloon injury. For therapeutic purposes they included fumagillin in the lipid monolayer of the nanoparticles and observed an anti-angiogenic effect with MRI that was confirmed histologically.

Lipoproteins

Low-density lipoprotein (LDL) and high-density lipoprotein (HDL) play an important role in the transport of cholesterol. LDL consists of a lipid core of cholesterol esters and triglycerides covered by a phospholipid monolayer which contains a large apolipoprotein. LDL binds to the LDL receptor exclusively via this apolipoprotein and is subsequently internalized. The overexpression of the LDL receptor is associated with several pathologies, including atherosclerosis and cancer. Hui *et al.* labeled LDL by incubating it with PTIR267 molecules (171), a contrast agent with a Gd–DTPA moiety and a fluorescent label. *In vitro* uptake of this contrast agent by melanoma cells was determined with fluorescence microscopy. *In vivo* they observed increased contrast in the mouse B16 melanoma tumors and in the mouse liver, whereas the uptake in the liver of LDL receptor knockout mice was very low.

An HDL-like particle was developed by Frias *et al.* for bimodal imaging (102). They constructed the particle from apo-HDL proteins and phospholipids, with or without unesterified cholesterol. A paramagnetic phospholipid, Gd–DTPA–DMPE and a fluorescent phospholipid were incorporated (Fig. 9) for imaging purposes. This contrast agent was tested on a mouse model of atherosclerosis that was imaged *in vivo* with MRI. The vessel wall of the abdominal aorta showed strong signal enhancement with a maximum 24 h post-injection. Following aorta excision, it was established with *post mortem* confocal fluorescence microscopy that the contrast agent was mainly localized in the intimal layer. The lipoprotein contrast agents may be of great use for the non-invasive characterization of cancer and atherosclerosis.

Smart contrast agents

Smart contrast agents, also referred to as responsive or activated contrast agents, are agents that undergo a large change in relaxivity upon activation. A key study in this field was published by Louie *et al* (16). They developed a Gd^{3+} chelating complex, which, in the presence of the enzyme β-galactosidase, undergoes a sizable increase in

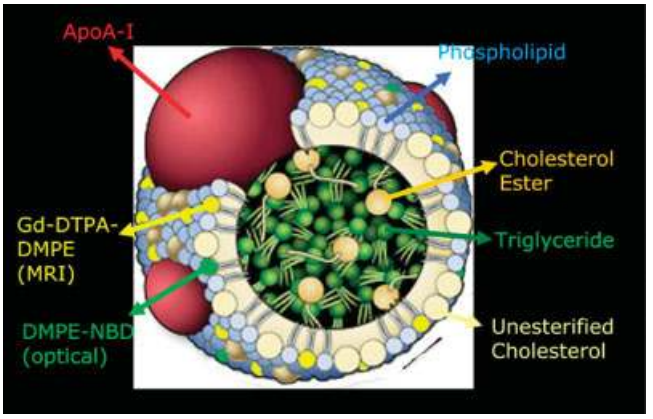

Figure 9. Different components of the recombinant HDL-like MRI contrast agent. Adapted from Scheme 1 of Frias *et al.*, Recombinant HDL-like nanoparticles: a specific contrast agent for MRI of atherosclerotic plaques. *J. Am. Chem. Soc.* 2004; **126**: 16316–16327, with permission from the American Chemical Society

relaxivity. In its inactive form water is not accessible to Gd^{3+} because of blockage with a sugar moiety. When the enzyme cleaves off the sugar water can directly coordinate with Gd^{3+} explaining the r_1 increase. Peroxidase activity has been detected with MRI by using iron oxide nanoparticles conjugated with phenolic molecules that crosslink in the presence of peroxidases. This leads to the self-assembly of the nanoparticles (172), which results in a concentration-dependent decrease of T_2.

Liposomes have also been used as smart contrast material. Liposomes can, for example, be prepared to undergo a phase transition of the bilayer following a physiological trigger. When the bilayer is in a rigid, gel-like state, it is poorly permeable to water. After the phase transition, the membrane becomes more fluid and hence more permeable to water. The phase transition can be caused by, e.g., pH changes or temperature changes. Gd–DTPA–BMA encapsulated by pH-sensitive liposomes composed of phosphatidylethanolamine and palmitic acid were studied by Lokling *et al.* (127). The use of these liposomes was initially limited because of their low stability in blood (173). Exchanging palmitic acid for the double-chained amphiphile dipalmitoylglycerosuccinate resulted in a formulation with increased stability and good pH sensitivity (174). This contrast agent might be useful for pH quantification, which is clinically relevant for characterizing tumors.

Similar liposomal systems have been used in several studies for the non-invasive determination of local temperature (114). The relaxivity of these liposomes increases when the temperature is above the gel-to-liquid crystalline phase transition. Frich *et al.* used thermosensitive liposomes for image-guided thermal ablation of rabbit liver (126). Upon heating, an increase in tissue signal was observed in T_1-weighted images (Fig. 10), thus allowing on-line monitoring of thermal ablation.

Another example of a smart imaging strategy is to determine drug release from liposomes using MRI (125). $MnSO_4$- and doxorubicin-loaded liposomes were used for monitoring the release of the drug from the liposomes with MRI. Mn^{2+} is a paramagnetic ion which shortens the T_1 of water. However, when Mn^{2+} is encapsulated in liposomes the relaxivity decreases dramatically. The release of content from temperature-sensitive liposomes could be followed by the increase in the MRI signal in T_1-weighted images.

A liposomal contrast agent responsive to radicals has also been described (175). In this agent, Gd^{3+} chelates are conjugated to the liposome via a disulfide linker. The rotational correlation time of this conjugate is long, resulting in a high relaxivity. When the contrast agent is exposed to radicals, the paramagnetic chelates are cleaved off, leading to faster tumbling and a corresponding decrease in the relaxivity.

Cell labeling

MRI as a cellular imaging modality depends on methods to label magnetically cells of interest in order to monitor their trafficking as part of cell-based repair, replacement and treatment strategies. Efficient magnetic labeling of the cells to be tracked with MRI is of great importance for keeping the detection limit of the cells as low as possible. The migration of magnetically-labeled implanted stem cells was successfully monitored in the brain of experimental stroke rats by Hoehn *et al.* (176) and in a myocardial infarction pig model by Kraitchman *et al.* (177)

Different strategies have been described that mainly focus on loading cells with iron oxide particles. In an early study performed by Bulte *et al.*, liposomes containing dextran-coated iron oxide particles were used for labeling of human peripheral blood mononuclear cells with iron oxide particles (145). For efficient incorporation, transfection agents, originally developed to transfect non-viral DNA, may be used. Among the different transfection agents, a subgroup are the lipid-based transfection agents, usually cationic liposomes. Labeling cells with magnetic iron oxide particles can be done with high efficiency using these lipid-based transfection agents. Van den Bos *et al.*, for example, reported that the use of cationic liposomes for iron oxide stem cell labeling increased the labeling efficiency approximately 100-fold (178). The above methods introduce superparamagnetic properties to the cells. Efficient paramagnetic labeling of cells can be done with cationic liposomes (179) or microemulsions containing a high payload of an amphiphilic paramagnetic moiety. These systems can also carry a fluorescent lipid for simultaneous detection with fluorescence microscopy. Recently, perfluoropolyether-containing microemulsions have been used to label dendritic cells (180). The cells were tracked in mice

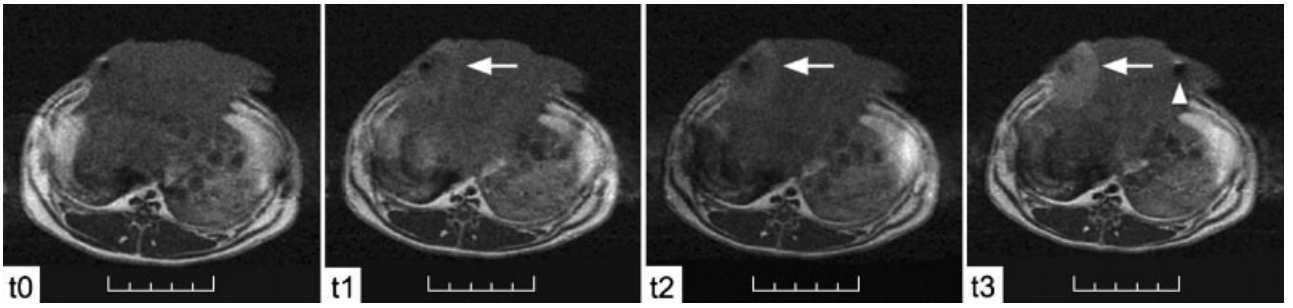

Figure 10. T_1-weighted images of radiofrequency ablation in rabbit liver after injection of liposomal contrast. Prior to heating (t0), during heating (t1), after normalization of tissue temperature (t2) and 15–20 min after normalization of tissue temperature (t3). Note the increasing signal intensity in the periphery of the thermal lesion in the right liver lobe (white arrows). The radiofrequency electrode has been repositioned in the left liver lobe at *t*3 (white arrowhead). Adapted from Fig. 4 of Frich *et al.*, Experimental application of thermosensitive paramagnetic liposomes for monitoring magnetic resonance imaging guided thermal ablation. *Magn. Reson. Med.* 2004; **52**: 1302–1309, with permission from John Wiley & Sons, Inc

in vivo using ^{19}F MRI. The main advantage of this technique is that it allows imaging of the cells without any background, so-called hot-spot imaging, since there are no endogenous fluorine atoms present in the body. The information obtained with ^{19}F MRI can be superimposed on high-resolution anatomical ^{1}H MR images, allowing accurate localization of the contrast material.

RECENT DEVELOPMENTS

In addition to MRI, lipidic nanoparticles have also been employed as contrast agents for other imaging modalities. Liposomes with appropriate radiolabels have been used for positron emission tomography (PET) (181), single photon emission computed tomography (SPECT) (182) and scintigraphy imaging (183). For computed tomography (CT), liposomes can carry heavily iodinated organic compounds, whereas for ultrasound the liposomes should be echogenic (184). Micelles with an amphiphilic indium-111-labeled moiety have been applied for lymphography (33). In addition to the established utility of perfluorocarbon nanoparticles as ultrasonic and MRI contrast agents, this technology has been further modified for other imaging methods such as CT (185) and nuclear techniques. Such multimodal nanoparticles may be of use in choosing the optimal detection or imaging method with the same nanoparticulate probe. Furthermore, a combinatory approach may be beneficial for improved detection. A sensitive and low-resolution technique, such as the nuclear techniques, can provide information on the biodistribution of the nanoparticles. A whole body can be scanned and areas of interest can thus be identified relatively rapidly. Thereafter, these areas may be investigated in more detail with high-resolution and low-sensitivity techniques such as CT and MRI. The combination may also be of use to merge anatomical information from MRI or CT with the sensitive detection of the contrast agent with nuclear methods.

Quantum dots, semiconductor nanocrystals a few nanometers in size, have recently attracted much attention for biological imaging purposes (186) because of their excellent fluorescent properties, but their use has been limited by difficulties in obtaining quantum dots that are biocompatible. Quantum dots capped in phospholipid micelles (39) were among the first to be applied *in vivo*. Mulder *et al.* recently extended this approach by applying a paramagnetic lipidic coating to quantum dots for simultaneous detection with MRI (187).

Another promising application of nanoparticles is their use for combined diagnostics and treatment. As discussed previously, extensive research has been done with lipidic aggregates as pharmaceutical carriers, which makes the implementation of combining a MRI contrast agent with a therapeutic agent relatively easy.

CEST (chemical exchange saturation transfer) agents are agents that contain at least one pool of exchangeable protons, which upon irradiation at their resonance frequency transfer magnetization to the strong signal from bulk water. CEST agents are interesting because they can be switched on and off, but are limited because of their low sensitivity. Creating particles with a large number of exchangeable protons may be done with liposomes. This so-called LIPOCEST approach, which was recently proposed by Aime *et al.* (188), relies on the incorporation of an MR shift reagent in the liposomal lumen. This causes the resonance frequency of water protons inside the liposomes to be shifted from that of the external water. In a phantom study, the authors were able to detect the contrast agent at a concentration as low as 90 pM. Terreno *et al.* presented initial results of *in vitro* targeting of this LIPOCEST agent (189). In that study, the liposomes were coated with PEG and coupled to peptides via avidin–biotin bonding. In addition, MRI visualization of the passive accumulation of pegylated LIPOCEST in tumor-bearing mice was demonstrated.

CONCLUSIONS

In this review, we have shown the variety of possibilities of using lipids and other amphiphiles as building blocks of nanoparticulate MRI contrast agents. Phospholipids are the most commonly used amphiphiles for biomedical applications, which has resulted in the commercial availability of many different lipids and phospholipid-like structures. Magnetic resonance is a leading diagnostic imaging modality, since it excels in depicting soft tissue with high spatial resolution. Nevertheless, to improve the applicability of contrast-enhanced MRI, the limitations of the technique have to be taken into consideration. First, the relatively low sensitivity of MR can be compensated by creating highly potent contrast agents, which is possible by using lipidic particles with a high payload of contrast material. Second, although the spatial resolution of MRI is superior to that of other non-invasive *in vivo* imaging modalities, the level of detail that is obtained with immunohistochemical techniques will not be achieved. Therefore, in the initial phase MRI should be combined with a complementary imaging technique to gain more insight into the pathology studied and into the mechanisms of uptake and fate of the contrast agent. Fluorescence microscopy is such a technique, which is capable of studying processes with subcellular resolution. Fluorescence microscopy is mainly applied *post mortem* on small tissue sections, because of the limited penetration depth of light. The availability of fluorescent lipids provides opportunities to create easily bimodal contrast agents that can be detected with both MRI and fluorescence microscopy. Much is expected from this bimodal imaging approach and initial studies have already revealed promising possibilities.

Gd^{3+} as an MRI contrast agent has to be chelated in a complex with a high binding constant, because of its toxicity. The toxicity of Gd–DTPA is low and well documented. Gd–DTPA therefore is FDA approved and the most commonly used agent. It has a low molecular weight and is rapidly secreted by the kidneys. Gd–DTPA-based contrast agents of high molecular weight have prolonged circulation times and accumulate at specific sites. Future studies have to reveal whether this causes any adverse health effects and whether lipidic nanoparticulate contrast agents can be used safely and cost-effectively in humans.

The ease of preparation, the flexibility and, most importantly, the biocompatibility of lipidic nanoparticles make them useful tools for biomedical imaging purposes. Lipidic nanoparticles also provide an excellent template for any new (molecular) MRI nanoparticle. Ongoing developments in nanotechnology (190–192) may lead to the development of nanoparticles for MRI with better relaxation properties, improved stability and a more defined size and structure.

REFERENCES

1. Haacke EM, Brown RW, Thompson MR, Venkatesan R. *Magnetic Resonance Imaging: Physical Principles and Sequence Design*. Wiley: New York, 1999.
2. Caravan P, Ellison JJ, McMurry TJ, Lauffer RB. Gadolinium(III) chelates as MRI contrast agents: structure, dynamics and applications. *Chem. Rev.* 1999; **99**: 2293–2352.
3. Aime S, Botta M, Fasano M, Terreno E. Lanthanide(III) chelates for NMR biomedical applications. *Chem. Soc. Rev.* 1998; **27**: 19–29.
4. Bulte JW, Kraitchman DL. Iron oxide MR contrast agents for molecular and cellular imaging. *NMR Biomed.* 2004; **17**: 484–499.
5. Lorenz CH, Johansson LO. Contrast-enhanced coronary MRA. *J. Magn. Reson. Imaging* 1999; **10**: 703–708.
6. Lutz AM, Seemayer C, Corot C, Gay RE, Goepfert K, Michel BA, Marincek B, Gay S, Weishaupt D. Detection of synovial macrophages in an experimental rabbit model of antigen-induced arthritis: ultrasmall superparamagnetic iron oxide-enhanced MR imaging. *Radiology* 2004; **233**: 149–157.
7. Padhani AR. Dynamic contrast-enhanced MRI in clinical oncology: current status and future directions. *J. Magn. Reson. Imaging* 2002; **16**: 407–422.
8. Dafni H, Gilead A, Nevo N, Eilam R, Harmelin A, Neeman M. Modulation of the pharmacokinetics of macromolecular contrast material by avidin chase: MRI, optical and inductively coupled plasma mass spectrometry tracking of triply labeled albumin. *Magn. Reson. Med.* 2003; **50**: 904–914.
9. Ruehm SG, Corot C, Vogt P, Kolb S, Debatin JF. Magnetic resonance imaging of atherosclerotic plaque with ultrasmall superparamagnetic particles of iron oxide in hyperlipidemic rabbits. *Circulation* 2001; **103**: 415–422.
10. Winter PM, Morawski AM, Caruthers SD, Fuhrhop RW, Zhang H, Williams TA, Allen JS, Lacy EK, Robertson JD, Lanza GM, Wickline SA. Molecular imaging of angiogenesis in early-stage atherosclerosis with alpha(v)beta3-integrin-targeted nanoparticles. *Circulation* 2003; **108**: 2270–2274.
11. Veldhuis WB, Floris S, van der Meide PH, Vos IM, de Vries HE, Dijkstra CD, Bar PR, Nicolay K. Interferon-beta prevents cytokine-induced neutrophil infiltration and attenuates blood-brain barrier disruption. *J Cereb Blood Flow Metab.* 2003; **23**: 1060–1069.
12. Weissleder R, Mahmood U. Molecular imaging. *Radiology* 2001; **219**: 316–333.
13. Kroft LJ, de Roos A. Blood pool contrast agents for cardiovascular MR imaging. *J. Magn. Reson. Imaging* 1999; **10**: 395–403.
14. de Lussanet QG, Langereis S, Beets-Tan RG, van Genderen MH, Griffioen AW, van Engelshoven JM, Backes WH. Dynamic contrast-enhanced MR imaging kinetic parameters and molecular weight of dendritic contrast agents in tumor angiogenesis in mice. *Radiology* 2005; **235**: 65–72.
15. Sipkins DA, Cheresh DA, Kazemi MR, Nevin LM, Bednarski MD, Li KC. Detection of tumor angiogenesis in vivo by alphaVbeta3-targeted magnetic resonance imaging. *Nat. Med.* 1998; **4**: 623–626.
16. Louie AY, Huber MM, Ahrens ET, Rothbacher U, Moats R, Jacobs RE, Fraser SE, Meade TJ. *In vivo* visualization of gene expression using magnetic resonance imaging. *Nat. Biotechnol.* 2000; **18**: 321–325.
17. Lewin M, Carlesso N, Tung CH, Tang XW, Cory D, Scadden DT, Weissleder R. Tat peptide-derivatized magnetic nanoparticles allow *in vivo* tracking and recovery of progenitor cells. *Nat. Biotechnol.* 2000; **18**: 410–414.
18. Crich SG, Biancone L, Cantaluppi V, Duo D, Esposito G, Russo S, Camussi G, Aime S. Improved route for the visualization of stem cells labeled with a Gd-/Eu-chelate as dual (MRI and fluorescence) agent. *Magn. Reson. Med.* 2004; **51**: 938–944.
19. Lukyanov AN, Torchilin VP. Micelles from lipid derivatives of water-soluble polymers as delivery systems for poorly soluble drugs. *Adv. Drug Deliv. Rev.* 2004; **56**: 1273–1289.
20. Torchilin VP. Targeted polymeric micelles for delivery of poorly soluble drugs. *Cell. Mol. Life Sci.* 2004; **61**: 2549–2559.

21. Allen TM. Long-circulating (sterically stabilized) liposomes for targeted drug delivery. *Trends Pharmacol. Sci.* 1994; **15**: 215–220.
22. Storm G, Crommelin DJA. Colloidal systems for tumor targeting. *Hybridoma* 1997; **16**: 119–125.
23. Torchilin VP. Recent advances with liposomes as pharmaceutical carriers. *Nat. Rev. Drug Discov.* 2005; **4**: 145–160.
24. Torchilin VP, Lukyanov AN, Gao Z, Papahadjopoulos-Sternberg B. Immunomicelles: targeted pharmaceutical carriers for poorly soluble drugs. *Proc. Natl. Acad. Sci. USA* 2003; **100**: 6039–6044.
25. Allen TM. Ligand-targeted therapeutics in anticancer therapy. *Nat. Rev. Cancer* 2002; **2**: 750–763.
26. Torchilin VP. Fluorescence microscopy to follow the targeting of liposomes and micelles to cells and their intracellular fate. *Adv. Drug Deliv. Rev.* 2005; **57**: 95–109.
27. Weissleder R, Mahmood U. Molecular imaging. *Radiology* 2001; **219**: 316–333.
28. Lanza GM, Winter PM, Caruthers SD, Morawski AM, Schmieder AH, Crowder KC, Wickline SA. Magnetic resonance molecular imaging with nanoparticles. *J. Nucl. Cardiol.* 2004; **11**: 733–743.
29. Raymond KN, Pierre VC. Next generation, high relaxivity gadolinium MRI agents. *Bioconjug. Chem.* 2005; **16**: 3–8.
30. Storrs RW, Tropper FD, Li HY, Song CK, Kuniyoshi JK, Sipkins DA, Li KCP, Bednarski MD. Paramagnetic polymerized liposomes – synthesis, characterization and applications for magnetic-resonance-imaging. *J. Am. Chem. Soc.* 1995; **117**: 7301–7306.
31. Mulder WJ, Strijkers GJ, Griffioen AW, van Bloois L, Molema G, Storm G, Koning GA, Nicolay K. A liposomal system for contrast-enhanced magnetic resonance imaging of molecular targets. *Bioconjug. Chem.* 2004; **15**: 799–806.
32. Morawski AM, Winter PM, Yu X, Fuhrhop RW, Scott MJ, Hockett F, Robertson JD, Gaffney PJ, Lanza GM, Wickline SA. Quantitative 'magnetic resonance immunohistochemistry' with ligand-targeted F-19 nanoparticles. *Magn. Reson. Med.* 2004; **52**: 1255–1262.
33. Torchilin VP. PEG-based micelles as carriers of contrast agents for different imaging modalities. *Adv. Drug Deliv. Rev.* 2002; **54**: 235–252.
34. Glogard C, Stensrud G, Hovland R, Fossheim SL, Klaveness J. Liposomes as carriers of amphiphilic gadolinium chelates: the effect of membrane composition on incorporation efficacy and *in vitro* relaxivity. *Int. J. Pharm.* 2002; **233**: 131–140.
35. Nitin N, Laconte LEW, Zurkiya O, Hu X, Bao G. Functionalization and peptide-based delivery of magnetic nanoparticles as an intracellular MRI contrast agent. *J. Biol. Inorg. Chem.* 2004; **9**: 706–712.
36. Degiorgio V. Physics of amphiphiles: micelles, vesicles and microemulsions. Amsterdam, 1985.
37. *Phospholipids Handbook*. Marcel Dekker: New York, 1993.
38. Lawrence MJ, Rees GD. Microemulsion-based media as novel drug delivery systems. *Adv. Drug Deliv. Rev.* 2000; **45**: 89–121.
39. Dubertret B, Skourides P, Norris DJ, Noireaux V, Brivanlou AH, Libchaber A. *In vivo* imaging of quantum dots encapsulated in phospholipid micelles. *Science* 2002; **298**: 1759–1762.
40. Bulte JW, De Cuyper M. Magnetoliposomes as contrast agents. *Methods Enzymol.* 2003; **373**: 175–198.
41. Johnsson M, Edwards K. Liposomes, disks and spherical micelles: aggregate structure in mixtures of gel phase phosphatidylcholines and poly(ethylene glycol)–phospholipids. *Biophys. J.* 2003; **85**: 3839–3847.
42. Drummond DC, Meyer O, Hong K, Kirpotin DB, Papahadjopoulos D. Optimizing liposomes for delivery of chemotherapeutic agents to solid tumors. *Pharmacol. Rev.* 1999; **51**: 691–743.
43. Lukyanov AN, Torchilin VP. Micelles from lipid derivatives of water-soluble polymers as delivery systems for poorly soluble drugs. *Adv. Drug Deliv. Rev.* 2004; **56**: 1273–1289.
44. Torchilin VP. Targeted polymeric micelles for delivery of poorly soluble drugs. *Cell. Mol. Life Sci.* 2004; **61**: 2549–2559.
45. Allen TM. Long-circulating (sterically stabilized) liposomes for targeted drug delivery. *Trends Pharmacol. Sci.* 1994; **15**: 215–220.
46. Park JW. Liposome-based drug delivery in breast cancer treatment. *Breast Cancer Res* 2002; **4**: 95–99.
47. O'Shaughnessy JA. Pegylated liposomal doxorubicin in the treatment of breast cancer. *Clin Breast Cancer* 2003; **4**: 318–328.
48. Torchilin VP. Recent advances with liposomes as pharmaceutical carriers. *Nat. Rev. Drug Discov.* 2005; **4**: 145–160.
49. Allen TM. Liposomes. Opportunities in drug delivery. *Drugs* 1997; **54**(Suppl. 4): 8–14.
50. Storm G, Crommelin DJ. Colloidal systems for tumor targeting. *Hybridoma* 1997; **16**: 119–125.
51. Tardi PG, Boman NL, Cullis PR. Liposomal doxorubicin. *J. Drug Target.* 1996; **4**: 129–140.
52. Kim ES, Lu C, Khuri FR, Tonda M, Glisson BS, Liu D, Jung M, Hong WK, Herbst RS. A phase II study of STEALTH cisplatin (SPI-77) in patients with advanced non-small cell lung cancer. *Lung Cancer* 2001; **34**: 427–432.
53. Burger KN, Staffhorst RW, de Vijlder HC, Velinova MJ, Bomans PH, Frederik PM, de Kruijff B. Nanocapsules: lipid-coated aggregates of cisplatin with high cytotoxicity. *Nat. Med.* 2002; **8**: 81–84.
54. Klibanov AL, Maruyama K, Torchilin VP, Huang L. Amphipathic polyethyleneglycols effectively prolong the circulation time of liposomes. *FEBS Lett.* 1990; **268**: 235–237.
55. Allen TM, Hansen C, Martin F, Redemann C, Yau-Young A. Liposomes containing synthetic lipid derivatives of poly(ethylene glycol) show prolonged circulation half-lives *in vivo*. *Biochim. Biophys. Acta* 1991; **1066**: 29–36.
56. Allen TM, Hansen C. Pharmacokinetics of stealth versus conventional liposomes: effect of dose. *Biochim. Biophys. Acta* 1991; **1068**: 133–141.
57. Torchilin VP. Targeted polymeric micelles for delivery of poorly soluble drugs. *Cell. Mol. Life Sci.* 2004; **61**: 2549–2559.
58. Jones M, Leroux J. Polymeric micelles – a new generation of colloidal drug carriers. *Eur. J. Pharm. Biopharm.* 1999; **48**: 101–111.
59. Bagwe RP, Kanicky JR, Palla BJ, Patanjali PK, Shah DO. Improved drug delivery using microemulsions: rationale, recent progress and new horizons. *Crit. Rev. Ther. Drug Carrier Syst.* 2001; **18**: 77–140.
60. Mastrobattista E, Koning GA, Storm G. Immunoliposomes for the targeted delivery of antitumor drugs. *Adv. Drug Deliv. Rev.* 1999; **40**: 103–127.
61. Koning GA, Schiffelers RM, Storm G. Endothelial cells at inflammatory sites as target for therapeutic intervention. *Endothelium* 2002; **9**: 161–171.
62. Torchilin VP, Lukyanov AN, Gao Z, Papahadjopoulos-Sternberg B. Immunomicelles: targeted pharmaceutical carriers for poorly soluble drugs. *Proc. Natl. Acad. Sci. USA* 2003; **100**: 6039–6044.
63. Sapra P, Allen TM. Ligand-targeted liposomal anticancer drugs. *Prog. Lipid Res.* 2003; **42**: 439–462.
64. Torchilin VP. Recent advances with liposomes as pharmaceutical carriers. *Nat. Rev. Drug Discov.* 2005; **4**: 145–160.
65. Klibanov AL, Maruyama K, Torchilin VP, Huang L. Amphipathic polyethyleneglycols effectively prolong the circulation time of liposomes. *FEBS Lett.* 1990; **268**: 235–237.
66. Rensen PC, Schiffelers RM, Versluis AJ, Bijsterbosch MK, Kuijk-Meuwissen ME, Van Berkel TJ. Human recombinant apolipoprotein E-enriched liposomes can mimic low-density lipoproteins as carriers for the site-specific delivery of antitumor agents. *Mol. Pharmacol.* 1997; **52**: 445–455.
67. Holig P, Bach M, Volkel T, Nahde T, Hoffmann S, Muller R, Kontermann RE. Novel RGD lipopeptides for the targeting of liposomes to integrin-expressing endothelial and melanoma cells. *Protein Eng. Des. Sel.* 2004; **17**: 433–441.
68. Hood JD, Bednarski M, Frausto R, Guccione S, Reisfeld RA, Xiang R, Cheresh DA. Tumor regression by targeted gene delivery to the neovasculature. *Science* 2002; **296**: 2404–2407.
69. Winter PM, Caruthers SD, Kassner A, Harris TD, Chinen LK, Allen JS, Lacy EK, Zhang HY, Robertson JD, Wickline SA, Lanza GM. Molecular imaging of angiogenesis in nascent vx-2 rabbit tumors using a novel alpha (v)beta(3)-targeted nanoparticle and 1.5 tesla magnetic resonance imaging. *Cancer Res.* 2003; **63**: 5838–5843.

70. Bulte JW, Hoekstra Y, Kamman RL, Magin RL, Webb AG, Briggs RW, Go KG, Hulstaert CE, Miltenyi S, The TH. Specific MR imaging of human lymphocytes by monoclonal antibody-guided dextran-magnetite particles. *Magn. Reson. Med.* 1992; **25**: 148–157.
71. Sipkins DA, Gijbels K, Tropper FD, Bednarski M, Li KC, Steinman L. ICAM-1 expression in autoimmune encephalitis visualized using magnetic resonance imaging. *J. Neuroimmunol.* 2000; **104**: 1–9.
72. Flacke S, Fischer S, Scott MJ, Fuhrhop RJ, Allen JS, McLean M, Winter P, Sicard GA, Gaffney PJ, Wickline SA, Lanza GM. Novel MRI contrast agent for molecular imaging of fibrin implications for detecting vulnerable plaques. *Circulation* 2001; **104**: 1280–1285.
73. Phillips NC, Gagne L, Tsoukas C, Dahman J. Immunoliposome targeting to murine CD4+ leucocytes is dependent on immune status. *J. Immunol.* 1994; **152**: 3168–3174.
74. Paganelli G, Pervez S, Siccardi AG, Rowlinson G, Deleide G, Chiolerio F, Malcovati M, Scassellati GA, Epenetos AA. Intraperitoneal radio-localization of tumors pre-targeted by biotinylated monoclonal antibodies. *Int. J. Cancer* 1990; **45**: 1184–1189.
75. Coussens LM, Werb Z. Inflammation and cancer. *Nature* 2002; **420**: 860–867.
76. Libby P. Inflammation in atherosclerosis. *Nature* 2002; **420**: 868–874.
77. Libby P, Ridker PM, Maseri A. Inflammation and atherosclerosis. *Circulation* 2002; **105**: 1135–1143.
78. Nathan C. Points of control in inflammation. *Nature* 2002; **420**: 846–852.
79. Kooi ME, Cappendijk VC, Cleutjens KB, Kessels AG, Kitslaar PJ, Borgers M, Frederik PM, Daemen MJ, van Engelshoven JM. Accumulation of ultrasmall superparamagnetic particles of iron oxide in human atherosclerotic plaques can be detected by *in vivo* magnetic resonance imaging. *Circulation* 2003; **107**: 2453–2458.
80. Kircher MF, Allport JR, Graves EE, Love V, Josephson L, Lichtman AH, Weissleder R. *In vivo* high resolution three-dimensional imaging of antigen-specific cytotoxic T-lymphocyte trafficking to tumors. *Cancer Res.* 2003; **63**: 6838–6846.
81. Barkhausen J, Ebert W, Heyer C, Debatin JF, Weinmann HJ. Detection of atherosclerotic plaque with gadofluorine-enhanced magnetic resonance imaging. *Circulation* 2003; **108**: 605–609.
82. Griffioen AW, Molema G. Angiogenesis: potentials for pharmacologic intervention in the treatment of cancer, cardiovascular diseases and chronic inflammation. *Pharmacol Rev.* 2000; **52**: 237–268.
83. Carmeliet P, Jain RK. Angiogenesis in cancer and other diseases. *Nature* 2000; **407**: 249–257.
84. Griffioen AW, Coenen MJ, Damen CA, Hellwig SM, van Weering DH, Vooys W, Blijham GH, Groenewegen G. CD44 is involved in tumor angiogenesis; an activation antigen on human endothelial cells. *Blood* 1997; **90**: 1150–1159.
85. Haubner R, Wester HJ, Weber WA, Mang C, Ziegler SI, Goodman SL, Senekowitsch-Schmidtke R, Kessler H, Schwaiger M. Noninvasive imaging of alpha(v)beta3 integrin expression using ^{18}F-labeled RGD-containing glycopeptide and positron emission tomography. *Cancer Res.* 2001; **61**: 1781–1785.
86. Koopman G, Reutelingsperger CP, Kuijten GA, Keehnen RM, Pals ST, van Oers MH. Annexin V for flow cytometric detection of phosphatidylserine expression on B cells undergoing apoptosis. *Blood* 1994; **84**: 1415–1420.
87. Blankenberg FG, Katsikis PD, Tait JF, Davis RE, Naumovski L, Ohtsuki K, Kopiwoda S, Abrams MJ, Darkes M, Robbins RC, Maecker HT, Strauss HW. *In vivo* detection and imaging of phosphatidylserine expression during programmed cell death. *Proc. Natl. Acad. Sci. USA* 1998; **95**: 6349–6354.
88. Hofstra L, Liem IH, Dumont EA, Boersma HH, van Heerde WL, Doevendans PA, De Muinck E, Wellens HJ, Kemerink GJ, Reutelingsperger CP, Heidendal GA. Visualisation of cell death *in vivo* in patients with acute myocardial infarction. *Lancet* 2000; **356**: 209–212.
89. Dumont EA, Reutelingsperger CP, Smits JF, Daemen MJ, Doevendans PA, Wellens HJ, Hofstra L. Real-time imaging of apoptotic cell-membrane changes at the single-cell level in the beating murine heart. *Nat. Med.* 2001; **7**: 1352–1355.
90. Petrovsky A, Schellenberger E, Josephson L, Weissleder R, Bogdanov A Jr. Near-infrared fluorescent imaging of tumor apoptosis. *Cancer Res.* 2003; **63**: 1936–1942.
91. Schellenberger EA, Sosnovik D, Weissleder R, Josephson L. Magneto/optical annexin V, a multimodal protein. *Bioconjug. Chem.* 2004; **15**: 1062–1067.
92. Jung HI, Kettunen MI, Davletov B, Brindle KM. Detection of apoptosis using the C2A domain of synaptotagmin I. *Bioconjug. Chem.* 2004; **15**: 983–987.
93. Zhao M, Beauregard DA, Loizou L, Davletov B, Brindle KM. Non-invasive detection of apoptosis using magnetic resonance imaging and a targeted contrast agent. *Nat. Med.* 2001; **7**: 1241–1244.
94. Niehans GA, Singleton TP, Dykoski D, Kiang DT. Stability of HER-2/neu expression over time and at multiple metastatic sites. *J. Natl. Cancer Inst.* 1993; **85**: 1230–1235.
95. Baselga J, Arteaga CL. Critical update and emerging trends in epidermal growth factor receptor targeting in cancer. *J. Clin. Oncol.* 2005; **23**: 2445–2459.
96. Park JW, Benz CC, Martin FJ. Future directions of liposome- and immunoliposome-based cancer therapeutics. *Semin. Oncol.* 2004; **31**: 196–205.
97. Artemov D, Mori N, Ravi R, Bhujwalla ZM. Magnetic resonance molecular imaging of the HER-2/neu receptor. *Cancer Res.* 2003; **63**: 2723–2727.
98. Park JW, Hong K, Kirpotin DB, Colbern G, Shalaby R, Baselga J, Shao Y, Nielsen UB, Marks JD, Moore D, Papahadjopoulos D, Benz CC. Anti-HER2 immunoliposomes: enhanced efficacy attributable to targeted delivery. *Clin. Cancer Res.* 2002; **8**: 1172–1181.
99. Glass CK, Witztum JL. Atherosclerosis. the road ahead. *Cell* 2001; **104**: 503–516.
100. Lusis AJ. Atherosclerosis. *Nature* 2000; **407**: 233–241.
101. Choudhury RP, Fuster V, Fayad ZA. Molecular, cellular and functional imaging of atherothrombosis. *Nat. Rev. Drug Discov.* 2004; **3**: 913–925.
102. Frias JC, Williams KJ, Fisher EA, Fayad ZA. Recombinant HDL-like nanoparticles: a specific contrast agent for MRI of atherosclerotic plaques. *J. Am. Chem. Soc.* 2004; **126**: 16316–16317.
103. Li H, Gray BD, Corbin I, Lebherz C, Choi H, Lund-Katz S, Wilson JM, Glickson JD, Zhou R. MR and fluorescent imaging of low-density lipoprotein receptors. *Acad. Radiol.* 2004; **11**: 1251–1259.
104. Kelly KA, Allport JR, Tsourkas A, Shinde-Patil VR, Josephson L, Weissleder R. Detection of vascular adhesion molecule-1 expression using a novel multimodal nanoparticle. *Circ. Res.* 2005; **96**: 327–336.
105. Johansson LO, Bjornerud A, Ahlstrom HK, Ladd DL, Fujii DK. A targeted contrast agent for magnetic resonance imaging of thrombus: implications of spatial resolution. *J. Magn. Reson. Imaging* 2001; **13**: 615–618.
106. Bangham AD, Standish MM, Watkins JC. Diffusion of univalent ions across the lamellae of swollen phospholipids. *J. Mol. Biol.* 1965; **13**: 238–252.
107. Torchilin VP. Recent advances with liposomes as pharmaceutical carriers. *Nat. Rev. Drug Discov.* 2005; **4**: 145–160.
108. Magin RL, Wright SM, Niesman MR, Chan HC, Swartz HM. Liposome delivery of NMR contrast agents for improved tissue imaging. *Magn. Reson. Med.* 1986; **3**: 440–447.
109. Koenig SH, Brown RD III, Kurland R, Ohki S. Relaxivity and binding of Mn^{2+} ions in solutions of phosphatidylserine vesicles. *Magn. Reson. Med.* 1988; **7**: 133–142.
110. Devoisselle JM, Vion-Dury J, Galons JP, Confort-Gouny S, Coustaut D, Canioni P, Cozzone PJ. Entrapment of gadolinium–DTPA in liposomes. Characterization of vesicles by P-31 NMR spectroscopy. *Invest. Radiol.* 1988; **23**: 719–724.
111. Unger E, Needleman P, Cullis P, Tilcock C. Gadolinium–DTPA liposomes as a potential MRI contrast agent. Work in progress. *Invest. Radiol.* 1988; **23**: 928–932.

112. Tilcock C, Unger E, Cullis P, MacDougall P. Liposomal Gd–DTPA: preparation and characterization of relaxivity. *Radiology* 1989; **171**: 77–80.
113. Caride VJ, Sostman HD, Winchell RJ, Gore JC. Relaxation enhancement using liposomes carrying paramagnetic species. *Magn. Reson. Imaging* 1984; **2**: 107–112.
114. Fossheim SL, Il'yasov KA, Hennig J, Bjornerud A. Thermosensitive paramagnetic liposomes for temperature control during MR imaging-guided hyperthermia: in vitro feasibility studies. *Acad. Radiol.* 2000; **7**: 1107–1115.
115. Fossheim SL, Fahlvik AK, Klaveness J, Muller RN. Paramagnetic liposomes as MRI contrast agents: influence of liposomal physicochemical properties on the in vitro relaxivity. *Magn. Reson. Imaging* 1999; **17**: 83–89.
116. Navon G, Panigel R, Valensin G. Liposomes containing paramagnetic macromolecules as MRI contrast agents. *Magn. Reson. Med.* 1986; **3**: 876–880.
117. Unger EC, Winokur T, MacDougall P, Rosenblum J, Clair M, Gatenby R, Tilcock C. Hepatic metastases: liposomal Gd–DTPA-enhanced MR imaging. *Radiology* 1989; **171**: 81–85.
118. Niesman MR, Bacic GG, Wright SM, Swartz HJ, Magin RL. Liposome encapsulated $MnCl_2$ as a liver specific contrast agent for magnetic resonance imaging. *Invest. Radiol.* 1990; **25**: 545–551.
119. Unger E, Fritz T, Shen DK, Wu G. Manganese-based liposomes. Comparative approaches. *Invest. Radiol.* 1993; **28**: 933–938.
120. Saito R, Bringas JR, McKnight TR, Wendland MF, Mamot C, Drummond DC, Kirpotin DB, Park JW, Berger MS, Bankiewicz KS. Distribution of liposomes into brain and rat brain tumor models by convection-enhanced delivery monitored with magnetic resonance imaging. *Cancer Res.* 2004; **64**: 2572–2579.
121. Mamot C, Nguyen JB, Pourdehnad M, Hadaczek P, Saito R, Bringas JR, Drummond DC, Hong K, Kirpotin DB, McKnight T, Berger MS, Park JW, Bankiewicz KS. Extensive distribution of liposomes in rodent brains and brain tumors following convection-enhanced delivery. *J. Neurooncol.* 2004; **68**: 1–9.
122. Heverhagen JT, Graser A, Fahr A, Muller R, Alfke H. Encapsulation of gadobutrol in AVE-based liposomal carriers for MR detectability. *Magn. Reson. Imaging* 2004; **22**: 483–487.
123. Unger E, Shen DK, Wu GL, Fritz T. Liposomes as MR contrast agents: pros and cons. *Magn. Reson. Med.* 1991; **22**: 304–308.
124. Koenig SH, Ahkong QF, Brown RD III, Lafleur M, Spiller M, Unger E, Tilcock C. Permeability of liposomal membranes to water: results from the magnetic field dependence of T1 of solvent protons in suspensions of vesicles with entrapped paramagnetic ions. *Magn. Reson. Med.* 1992; **23**: 275–286.
125. Viglianti BL, Abraham SA, Michelich CR, Yarmolenko PS, MacFall JR, Bally MB, Dewhirst MW. *In vivo* monitoring of tissue pharmacokinetics of liposome/drug using MRI: illustration of targeted delivery. *Magn. Reson. Med.* 2004; **51**: 1153–1162.
126. Frich L, Bjornerud A, Fossheim S, Tillung T, Gladhaug I. Experimental application of thermosensitive paramagnetic liposomes for monitoring magnetic resonance imaging guided thermal ablation. *Magn. Reson. Med.* 2004; **52**: 1302–1309.
127. Lokling KE, Fossheim SL, Skurtveit R, Bjornerud A, Klaveness J. pH-sensitive paramagnetic liposomes as MRI contrast agents: *in vitro* feasibility studies. *Magn. Reson. Imaging* 2001; **19**: 731–738.
128. Kabalka GW, Davis MA, Buonocore E, Hubner K, Holmberg E, Huang L. Gd-labeled liposomes containing amphipathic agents for magnetic resonance imaging. *Invest. Radiol.* 1990; **25**(Suppl. 1): S63–S64.
129. Kabalka GW, Buonocore E, Hubner K, Davis M, Huang L. Gadolinium-labeled liposomes containing paramagnetic amphipathic agents: targeted MRI contrast agents for the liver. *Magn. Reson. Med.* 1988; **8**: 89–95.
130. Kim SK, Pohost GM, Elgavish GA. Fatty-acyl iminopolycarboxylates: lipophilic bifunctional contrast agents for NMR imaging. *Magn. Reson. Med.* 1991; **22**: 57–67.
131. Schwendener RA, Wuthrich R, Duewell S, Wehrli E, von Schulthess GK. A pharmacokinetic and MRI study of unilamellar gadolinium–, manganese– and iron–DTPA–stearate liposomes as organ-specific contrast agents. *Invest. Radiol.* 1990; **25**: 922–932.
132. Tilcock C, Ahkong QF, Koenig SH, Brown RD III, Davis M, Kabalka G. The design of liposomal paramagnetic MR agents: effect of vesicle size upon the relaxivity of surface-incorporated lipophilic chelates. *Magn. Reson. Med.* 1992; **27**: 44–51.
133. Kabalka GW, Davis MA, Holmberg E, Maruyama K, Huang L. Gadolinium-labeled liposomes containing amphiphilic Gd–DTPA derivatives of varying chain length: targeted MRI contrast enhancement agents for the liver. *Magn. Reson. Imaging* 1991; **9**: 373–377.
134. Kabalka GW, Davis MA, Moss TH, Buonocore E, Hubner K, Holmberg E, Maruyama K, Huang L. Gadolinium-labeled liposomes containing various amphiphilic Gd–DTPA derivatives: targeted MRI contrast enhancement agents for the liver. *Magn. Reson. Med.* 1991; **19**: 406–415.
135. Hovland R, Glogard C, Aasen AJ, Klaveness J. Preparation and *in vitro* evaluation of a novel amphiphilic GdPCTA-[12] derivative; a micellar MRI contrast agent. *Org. Biomol. Chem.* 2003; **1**: 644–647.
136. Trubetskoy VS, Cannillo JA, Milshtein A, Wolf GL, Torchilin VP. Controlled delivery of Gd-containing liposomes to lymph nodes: surface modification may enhance MRI contrast properties. *Magn. Reson. Imaging* 1995; **13**: 31–37.
137. Bertini I, Bianchini F, Calorini L, Colagrande S, Fragai M, Franchi A, Gallo O, Gavazzi C, Luchinat C. Persistent contrast enhancement by sterically stabilized paramagnetic liposomes in murine melanoma. *Magn. Reson. Med.* 2004; **52**: 669–672.
138. Chu WJ, Simor T, Elgavish GA. *In vivo* characterization of Gd(BME–DTTA), a myocardial MRI contrast agent: tissue distribution of its MRI intensity enhancement and its effect on heart function. *NMR Biomed.* 1997; **10**: 87–92.
139. Leclercq F, Cohen-Ohana M, Mignet N, Sbarbati A, Herscovici J, Scherman D, Byk G. Design, synthesis and evaluation of gadolinium cationic lipids as tools for biodistribution studies of gene delivery complexes. *Bioconjug. Chem.* 2003; **14**: 112–119.
140. Storrs RW, Tropper FD, Li HY, Song CK, Sipkins DA, Kuniyoshi JK, Bednarski MD, Strauss HW, Li KC. Paramagnetic polymerized liposomes as new recirculating MR contrast agents. *J. Magn. Reson. Imaging* 1995; **5**: 719–724.
141. De Cuyper M, Joniau M. Potentialities of magnetoliposomes in studying symmetric and asymmetric phospholipid transfer processes. *Biochim. Biophys. Acta* 1990; **1027**: 172–178.
142. Margolis LB, Namiot VA, Kljukin LM. Magnetoliposomes: another principle of cell sorting. *Biochim. Biophys. Acta* 1983; **735**: 193–195.
143. Babincova M, Altanerova V, Lampert M, Altaner C, Machova E, Sramka M, Babinec P. Site-specific *in vivo* targeting of magnetoliposomes using externally applied magnetic field. *Z. Naturforsch. C* 2000; **55**: 278–281.
144. Babincova M, Leszczynska D, Sourivong P, Babinec P, Leszczynski J. Principles of magnetodynamic chemotherapy. *Med. Hypotheses* 2004; **62**: 375–377.
145. Bulte JW, Ma LD, Magin RL, Kamman RL, Hulstaert CE, Go KG, The TH, de Leij L. Selective MR imaging of labeled human peripheral blood mononuclear cells by liposome mediated incorporation of dextran-magnetite particles. *Magn. Reson. Med.* 1993; **29**: 32–37.
146. Martina MS, Fortin JP, Menager C, Clement O, Barratt G, Grabielle-Madelmont C, Gazeau F, Cabuil V, Lesieur S. Generation of superparamagnetic liposomes revealed as highly efficient MRI contrast agents for *in vivo* imaging. *J. Am. Chem. Soc.* 2005; **127**: 10676–10685.
147. De Cuyper M, Joniau M. Magnetoliposomes. Formation and structural characterization. *Eur. Biophys. J.* 1988; **15**: 311–319.
148. Bulte JW, De Cuyper M, Despres D, Frank JA. Short- vs. long-circulating magnetoliposomes as bone marrow-seeking MR contrast agents. *J. Magn. Reson. Imaging* 1999; **9**: 329–335.
149. Strijkers GJ, Mulder WJM, van Heeswijk RB, Frederik PM, Bomans P, Magusin PC, Nicolay K. Relaxivity of liposomal paramagentic MRI contrast agents. *MAGMA* 2005; **18**: 186–192.
150. van Tilborg GA, Strijkers GJ, Mulder WJ, Reutelingsperger CP, Nicolay K. AnnexinV-functionalized multimodal liposomes as

contrast agents for apoptotic cells. Proceedings of the 13th ISMRM Scientific Meeting 2005. Miami, FL, 2005.
151. Mulder WJ, Strijkers GJ, Habets JW, van der Schaft DW, Storm G, Koning GA, Griffioen AW, Nicolay K. MR Imaging of $\alpha v\beta 3$-expression in tumor bearing mice using RGD-conjugated paramagnetic and fluorescent liposomes [abstract]. *Angiogenesis* 2005; **2**: 183–184.
152. Mulder WJ, Strijkers GJ, Habets JW, Bleeker EJ, van der Schaft DW, Storm G, Koning GA, Griffioen AW, Nicolay K. MR molecular imaging and fluorescence microscopy for identification of activated tumor endothelium using a bimodal lipidic nanoparticle. *FASEB J.* 2005; **19**: 2008–2010.
153. Torchilin VP. Targeted polymeric micelles for delivery of poorly soluble drugs. *Cell. Mol. Life Sci.* 2004; **61**: 2549–2559.
154. Torchilin VP, Lukyanov AN, Gao Z, Papahadjopoulos-Sternberg B. Immunomicelles: targeted pharmaceutical carriers for poorly soluble drugs. *Proc. Natl. Acad. Sci. USA* 2003; **100**: 6039–6044.
155. Aime S, Barbero L, Botta M. Trends in NMR studies of paramagnetic Gd(III) complexes as potential contrast agents in MRI. *Magn. Reson. Imaging* 1991; **9**: 843–847.
156. Accardo A, Tesauro D, Roscigno P, Gianolio E, Paduano L, D'Errico G, Pedone C, Morelli G. Physicochemical properties of mixed micellar aggregates containing CCK peptides and Gd complexes designed as tumor specific contrast agents in MRI. *J. Am. Chem. Soc.* 2004; **126**: 3097–3107.
157. Amirbekian V, Lipinsk MJ, Frias JC, Aguinaldo JGS, Mani V, Fayad ZA. In vivo MR imaging of apolipoprotein-E knockout mice to detect atherosclerosis with gadolinium-containing micelles and immunomicelles molecularly targeted to macrophages. Proceedings of the 13th ISMRM Scientific Meeting 2005. Miami, FL, 2005.
158. Shimada M, Yoshikawa K, Suganuma T, Kayanuma H, Inoue Y, Ito K, Senoo A, Hayashi S. Interstitial magnetic resonance lymphography: comparative animal study of gadofluorine 8 and gadolinium diethylenetriamine-pentaacetic acid. *J. Comput.-Assist. Tomogr.* 2003; **27**: 641–646.
159. Misselwitz B, Platzek J, Raduchel B, Oellinger JJ, Weinmann HJ. Gadofluorine 8: initial experience with a new contrast medium for interstitial MR lymphography. *MAGMA* 1999; **8**: 190–195.
160. Misselwitz B, Platzek J, Weinmann HJ. Early MR lymphography with gadofluorine M in rabbits. *Radiology* 2004; **231**: 682–688.
161. Sirol M, Itskovich VV, Mani V, Aguinaldo JG, Weinmann HJ, Fuster V, Toussaint JF, Fayad ZA. Atherosclerotic plaque detection by contrast-enhanced magnetic resonance imaging. A comparative animal study of gadofluorine and Gd–DTPA. *Eur. Heart J.* 2004; **25**: 146.
162. Sirol M, Itskovich VV, Mani V, Aguinaldo JG, Fallon JT, Misselwitz B, Weinmann HJ, Fuster V, Toussaint JF, Fayad ZA. Lipid-rich atherosclerotic plaques detected by gadofluorine-enhanced *in vivo* magnetic resonance imaging. *Circulation* 2004; **109**: 2890–2896.
163. Sirol M, Moreno P, Fuster V, Weinmann HJ, Toussaint JF, Fayad ZA. Early versus advanced atherosclerotic plaque in vivo detection by gadofluorine-enhanced magnetic resonance imaging. *J. Am. Coll. Cardiol.* 2005; **45**: 297A.
164. Bendszus M, Wessig C, Schutz A, Horn T, Kleinschnitz C, Sommer C, Misselwitz B, Stoll G. Assessment of nerve degeneration by gadofluorine M-enhanced magnetic resonance imaging. *Ann. Neurol.* 2005; **57**: 388–395.
165. van Tilborg GA, Mulder WJ, Reutelingsperger CP, Strijkers GJ, Nicolay K. Imaging of apoptosis using targeted lipid-based bimodal contrast agents. Proceedings of the Fourth Annual Meeting of the Society for Molecular Imaging. Cologne, Germany: 2005.
166. Lanza GM, Wallace KD, Scott MJ, Cacheris WP, Abendschein DR, Christy DH, Sharkey AM, Miller JG, Gaffney PJ, Wickline SA. A novel site-targeted ultrasonic contrast agent with broad biomedical application. *Circulation* 1996; **94**: 3334–3340.
167. Lanza GM, Yu X, Winter PM, Abendschein DR, Karukstis KK, Scott MJ, Chinen LK, Fuhrhop RW, Scherrer DE, Wickline SA. Targeted antiproliferative drug delivery to vascular smooth muscle cells with a magnetic resonance imaging nanoparticle contrast agent implications for rational therapy of restenosis. *Circulation* 2002; **106**: 2842–2847.
168. Morawski AM, Winter PM, Crowder KC, Caruthers SD, Fuhrhop RW, Scott MJ, Robertson JD, Abendschein DR, Lanza GM, Wickline SA. Targeted nanoparticles for quantitative imaging of sparse molecular epitopes with MRI. *Magn. Reson. Med.* 2004; **51**: 480–486.
169. Winter PM, Morawski AM, Caruthers SD, Fuhrhop RW, Zhang HY, Williams TA, Allen JS, Lacy EK, Robertson JD, Lanza GM, Wickline SA. Molecular imaging of angiogenesis in early-stage atherosclerosis with alpha(v)beta(3)-integrin-targeted nanoparticles. *Circulation* 2003; **108**: 2270–2274.
170. Winter PM, Morawski AM, Caruthers SD, Harris TD, Fuhrhop RW, Zhang HY, Allen JS, Lacy EK, Williams TA, Wickline SA, Lanza GM. Antiangiogenic therapy of early atherosclerosis with paramagnetic alpha(v)beta(3)-integrin-targeted fumagillin nanoparticles. *J. Am. Coll. Cardiol.* 2004; **43**: 322A–323A.
171. Liu XN, Song L, Wang DW, Liao YH, Ma AQ, Zhu ZM, Zhao BR, Zhao JZ, Hui RT. [Correlation of thrombospondin-1 G1678A polymorphism to stroke: a study in Chinese population]. *Zhonghua Yi Xue Za Zhi* 2004; **84**: 1959–1962.
172. Perez JM, Simeone FJ, Tsourkas A, Josephson L, Weissleder R. Peroxidase substrate nanosensors for MR imaging. *Nano Lett.* 2004; **4**: 119–122.
173. Lokling KE, Skurtveit R, Fossheim SL, Smistad G, Henriksen I, Klaveness J. pH-sensitive paramagnetic liposomes for MRI: assessment of stability in blood. *Magn. Reson. Imaging* 2003; **21**: 531–540.
174. Lokling KE, Skurtveit R, Bjornerud A, Fossheim SL. Novel pH-sensitive paramagnetic liposomes with improved MR properties. *Magn. Reson. Med.* 2004; **51**: 688–696.
175. Glogard C, Stensrud G, Aime S. Novel radical-responsive MRI contrast agent based on paramagnetic liposomes. *Magn. Resonan. Chem.* 2003; **41**: 585–588.
176. Hoehn M, Kustermann E, Blunk J, Wiedermann D, Trapp T, Wecker S, Focking M, Arnold H, Hescheler J, Fleischmann BK, Schwindt W, Buhrle C. Monitoring of implanted stem cell migration *in vivo*: a highly resolved *in vivo* magnetic resonance imaging investigation of experimental stroke in rat. *Proc. Natl. Acad. Sci. USA* 2002; **99**: 16267–16272.
177. Kraitchman DL, Heldman AW, Atalar E, Amado LC, Martin BJ, Pittenger MF, Hare JM, Bulte JW. *In vivo* magnetic resonance imaging of mesenchymal stem cells in myocardial infarction. *Circulation* 2003; **107**: 2290–2293.
178. van den Bos EJ, Wagner A, Mahrholdt H, Thompson RB, Morimoto Y, Sutton BS, Judd RM, Taylor DA. Improved efficacy of stem cell labeling for magnetic resonance imaging studies by the use of cationic liposomes. *Cell Transplant.* 2003; **12**: 743–756.
179. Vuu K, Xie J, McDonald MA, Bernardo M, Hunter F, Zhang Y, Li K, Bednarski M, Guccione S. Gadolinium–rhodamine nanoparticles for cell labeling and tracking via magnetic resonance and optical imaging. *Bioconjug. Chem.* 2005; **16**: 995–999.
180. Ahrens ET, Flores R, Xu H, Morel PA. *In vivo* imaging platform for tracking immunotherapeutic cells. *Nat. Biotechnol.* 2005; **23**: 983–987.
181. Oku N. Delivery of contrast agents for positron emission tomography imaging by liposomes. *Adv. Drug Deliv. Rev.* 1999; **37**: 53–61.
182. Harrington KJ, Mohammadtaghi S, Uster PS, Glass D, Peters AM, Vile RG, Stewart JS. Effective targeting of solid tumors in patients with locally advanced cancers by radiolabeled pegylated liposomes. *Clin. Cancer Res.* 2001; **7**: 243–254.
183. Boerman OC, Laverman P, Oyen WJ, Corstens FH, Storm G. Radiolabeled liposomes for scintigraphic imaging. *Prog. Lipid Res.* 2000; **39**: 461–475.
184. Dagar S, Rubinstein I, Onyuksel H. Liposomes in ultrasound and gamma scintigraphic imaging. *Methods Enzymol.* 2003; **373**: 198–214.
185. Winter PM, Shukla HP, Caruthers SD, Scott MJ, Fuhrhop RW, Robertson JD, Gaffney PJ, Wickline SA, Lanza GM. Molecular imaging of human thrombus with computed tomography. *Acad. Radiol.* 2005; **12**(Suppl 1): S9–S13.
186. Michalet X, Pinaud FF, Bentolila LA, Tsay JM, Doose S, Li JJ, Sundaresan G, Wu AM, Gambhir SS, Weiss S. Quantum dots

for live cells, *in vivo* imaging and diagnostics. *Science* 2005; **307**: 538–544.
187. Mulder WJ, Koole R, Brandwijk RJ, Storm G, Chin PT, Strijkers GJ, de Mello Donega C, Nicolay K, Griffioen AW. Quantum Dots with a Paramagnetic Coating as a Bimodal Molecular Imaging Probe. Nano Lett 11-24-0005.
188. Aime S, Delli CD, Terreno E. Highly sensitive MRI chemical exchange saturation transfer agents using liposomes. *Angew. Chem. Int. Ed.* 2005; **44**: 5513–5515.
189. Terreno E, Castelli DD, Aime S. Towards highly-sensitive MRI-CEST agents. Cologne, 2005.
190. Ferrari M. Cancer nanotechnology: opportunities and challenges. *Nat. Rev. Cancer* 2005; **5**: 161–171.
191. Buxton DB, Lee SC, Wickline SA, Ferrari M. Recommendations of the National Heart, Lung and Blood Institute Nanotechnology Working Group. *Circulation* 2003; **108**: 2737–2742.
192. Moghimi SM, Hunter AC, Murray JC. Nanomedicine: current status and future prospects. *FASEB J.* 2005; **19**: 311–330.
193. Nicolle GM, Helm L, Merbach AE. S-8 paramagnetic centres in molecular assemblies: possible effect of their proximity on the water proton relaxivity. *Magn. Reson. Chem.* 2003; **41**: 794–799.
194. Winter PM, Caruthers SD, Yu X, Song SK, Chen JJ, Miller B, Bulte JWM, Robertson JD, Gaffney PJ, Wickline SA, Lanza GM. Improved molecular imaging contrast agent for detection of human thrombus. *Magn. Reson. Med.* 2003; **50**: 411–416.

